Similarities and Differences between the Mesomorphic Behaviour of Oligomeric Macrocyclics and of Linear High Relative Molecular Mass Polyethers based on 1-(4'-Hydroxybiphenyl-4-yl)-2-(4-hydroxyphenyl)butane and Flexible Spacers [1a]

Virgil Percec * and Masaya Kawasumi
Department of Macromolecular Science, Case Western Reserve University, Cleveland, OH 44106-2699, USA

This paper describes the synthesis and mesomorphic behaviour of macrocyclics of 1-(4'-hydroxybiphenyl-4-yl)-2-(4-hydroxyphenyl)butane (TPB) with α,ω-dibromoalkanes containing 13 [TPB-(*c*)13(*z*), where *z* defines the size of the macrocyclic, *i.e.*, *z* = 1, monomer; *z* = 2, dimer, *etc.*], 14 [TPB-(*c*)14(*z*)] and respectively 18 [TPB-(*c*)18(*z*)] methylenic groups. It also discusses the influence of spacer length, *x*, and ring size, *z*, on their NMR spectra and on the phase behaviour of TPB-(*c*)*x*(*z*) macrocyclics with *x* = 4–14 and 18, and with *z* = 1–5, in comparison with that of their linear high-relative-molecular-mass polyethers TPB-(*l*)*x*. Macrocyclic monomers are liquid, crystalline, or glassy. Only the macrocyclic dimers with *x* = 10 and 12–18 exhibit a monotropic nematic phase. The macrocyclic trimer with *x* = 6 displays a monotropic smectic phase. Those with *x* larger than 6 display an enantiotropic nematic phase, while those with *x* = 8, 13 and 14 exhibit, in addition to the enantiotropic nematic phase, also an enantiotropic smectic phase. Only the macrocyclic tetramer with *x* = 4 displays a monotropic nematic phase. All others exhibit enantiotropic nematic phases. All cyclic pentamers exhibit an enantiotropic nematic phase. The isotropization transition temperatures of cyclic trimers show an inverse odd–even dependence on *x* (*i.e.*, the higher temperature is displayed by odd spacers) while those of cyclic tetramers and pentamers show a conventional odd–even dependence. Owing to the higher rigidity of the macrocyclics than that of their linear low and high relative molecular mass homologues most macrocyclics exhibit higher isotropization temperatures than do even their corresponding high relative molecular mass linear derivatives. However, the enthalpy and entropy changes associated with the isotropization transitions of macrocyclics are lower than those of their linear high relative molecular mass homologues. These results demonstrate that macrocyclic compounds containing mesogenic groups represent a novel class of liquid crystals which displays a higher ability to form nematic and smectic phases than do the corresponding low and high relative molecular mass linear homologues.

Soon after the discovery of liquid crystals [1b] it was recognized that rigid linear and disc-like molecules provide the most suitable molecular architectures which lead to liquid crystalline mesophases.[1c] One hundred years later, the discussion on the molecular structure–properties relationship in the field of liquid crystals is still focused on the same two architectures and on few, less conventional variants of them.[1d–k] The same statement is valid for the field of macromolecular and supramolecular liquid crystals.[2] Recently, we have predicted and demonstrated that low-molar-mass macrocyclics based on conformationally flexible rod-like mesogens should and do exhibit a higher ability to generate liquid crystalline phases than do their low-molar-mass linear and both their linear and cyclic high relative molecular mass homologues[3] (Fig. 1). The trend outlined in Fig. 1 is due to the fact that macrocyclics of a certain size are more rigid than are the corresponding linear homologues as well as both their high molecular mass linear and cyclic compounds. At present, we are investigating the macrocyclic oligopolyethers of the conformationally flexible compound 1-(4-hydroxybiphenyl-4-yl)-2-(4-hydroxyphenyl)butane (TPB) with α,ω-dibromoalkanes[3] and comparing their phase behaviour with that of the corresponding linear polyethers.[4,5] Questions like: what is the shortest spacer and the minimum ring size of macrocyclic based on TPB which displays a liquid crystalline phase?;[3d] what is the lowest size of the macrocyclic which displays a liquid crystalline phase whose isotropization temperature is higher than that of its linear high relative molecular mass homologue?;[3a,d,f] what is the probability of transforming kinetically prohibited[3b] and/or kinetically controlled[3c] mesophases of the linear polymer into enantiotropic mesophases *via* cyclization?; and what is the ability to generate noncrystallizable macrocyclics with high glass transition temperature and a broad range of temperature of their mesophase?,[3e] were addressed and answered in our previous publications.

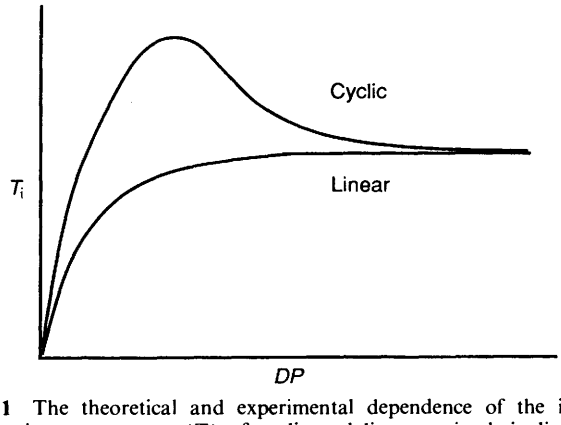

Fig. 1 The theoretical and experimental dependence of the isotropization temperature (T_i) of cyclic and linear main-chain liquid crystalline polymers on their degree of polymerization (*DP*). Both T_i and *DP* are in arbitrary units.

Although various classes of cyclic oligomers are generated

during both step condensations and ring-opening polymerizations,[6a-c] and are also important natural compounds such as ionophores,[7] cyclodextrins,[7b-c] DNA and peptides,[6c] there is very little understanding of the similarities and differences between cyclic and linear oligomers and polymers. This is mostly due to the difficult synthesis of cyclic oligomers[6d-f] and polymers.[6a-c,8-12] Previously, cyclic glassy oligomers and polymers, *i.e.*, polystyrene,[6a,b,8] polysiloxanes[6,9] and poly(2-vinylpyridine)[10] have been synthesized and characterized. Cyclic oligomers of polycarbonate[11] and of few other condensation polymers[12] have also been reported. Cyclic oligomers of polyethylene were prepared and used to allow us to understand the crystallization mechanism of polyethylene[6a,13] while cyclic side-chain crystalline oligomers and polymers have only recently been reported.[14] Probably the best investigated classes of macrocyclics are crown ethers, cryptands, calixarenes, and other cyclophanes which form host–guest complexes.[15] Recently, the interest centred around supramolecular chemistry[15c,d] has generated a great deal of activity in the area of complex architectures based on macrocyclics such as catenanes,[16a-c] rotaxanes,[16d,e,f] and knots.[16b,c] Macrocyclic liquid crystals are adding a new dimension to this entire field which so far has been concerned with liquid, glassy and crystalline states.

This paper has two goals. The first one is to describe the synthesis and mesomorphic behaviour of liquid crystalline macrocyclics based on TPB with α,ω-dibromoalkanes containing 13 [TPB-(*c*)13(*z*), where *z* defines the size of the macrocyclic, *i.e.*, *z* = 1 = monomer, 2 = dimer, *etc.*], 14 [TPB-(*c*)14(*z*)], and respectively 18 [TPB-(*c*)18(*z*)] methylenic groups. These are the last three groups of macrocyclics which complete the entire series of investigations on macrocyclics based on TPB and α,ω-dibromoalkanes containing from 4–14 and 18 methylenic groups. The second goal of this paper is to discuss the cyclization tendency of TPB with α,ω-dibromoalkanes as a function of spacer length, and to elucidate the similarities and differences between the spectroscopic and phase behaviour of macrocyclics and of their linear high-relative-molecular-mass homologues both as a function of spacer length and macrocyclic size (*i.e.*, degree of oligomerization).

Experimental

Materials.—Tetrabutylammonium hydrogen sulfate (TBAH) (97%, Aldrich) was used as received. 1,13-Dibromotridecane and 1,14-dibromotetradecane were synthesized as described in a previous publication and in papers cited therein.[17] 1,18-Dibromooctadecane (K and K Laboratories) was purified by recrystallization from methanol. *o*-Dichlorobenzene was distilled under reduced pressure. TPB (purity >99% by HPLC) was synthesized according to the previously described procedure.[4] Silica gel plates with fluorescent indicator (Eastman Kodak) were used for TLC analyses. All other chemicals were commercially available and were used as received.

Syntheses of Linear Polyethers TPB-(l)13, *TPB-*(l)14 *and TPB* -(l)18.—The linear polyether based on TPB and 1,13-dibromotridecane [TPB-(*l*)13] (M_n 32 900; M/M_n 2.08), the polyether based on TPB and 1,14-dibromotetradecane [TPB-(*l*)14] (M_n 30 200; M/M_n 2.16), and the polyether based on TPB and 1,18-dibromooctadecane [TPB-(*l*)18] (M_n 37 100, M/M_n 3.88) were synthesized by a liquid–liquid two-phase [*o*-dichlorobenzene/10 mol dm^{-3} aq. NaOH (10 times excess to the phenol groups)] phase-transfer-catalysed polymerization at high monomer concentration under nitrogen. Details of their syntheses, purification and characterization were presented elsewhere.[4]

Synthesis of Macrocyclic Oligoethers TPB-(c)13(z), *TPB-*(c)14(z), *and TPB-*(c)18(z) [*where* z = 1 (*monomer*), 2 (*dimer*), etc.].—The macrocyclics of TPB with 1,13-dibromotridecane, of TPB with 1,14-dibromotetradecane, and of TPB with 1,18-dibromooctadecane were synthesized by phase-transfer-catalysed polyetherification under high-dilution conditions [monomer (mmol)/solvent (cm^3) 1/100] under nitrogen at 80 °C in an *o*-dichlorobenzene–10 mol dm^{-3} NaOH mixture in the presence of TBAH as phase-transfer catalyst. After a reaction time of 40 h the reaction mixture was separated into the individual cyclic oligomers and the high relative molecular mass part. A general procedure used for the preparation of cyclic polyethers TPB-(*c*)13(*z*) is as follows.

To a 500 cm^3 single-neck flask equipped with a condenser were successively added TPB (0.478 g, 1.50 mmol), 1,13-dibromotridecane (0.513 g, 1.50 mmol), *o*-dichlorobenzene (150 cm^3), 10 mol dm^{-3} aq. NaOH (150 cm^3) and TBAH (0.204 g, 0.60 mmol). A balloon filled with nitrogen was placed at the top of the condenser. The reaction mixture, heated to 80 °C, was stirred at 1100 rpm with a magnetic stirrer. After 40 h, the reaction mixture was diluted with water and chloroform. The organic layer was washed twice with water, once with dil. hydrochloric acid, and three times with water. After evaporation of the solvents, the product was dissolved in chloroform. To this solution was added silica gel and the chloroform was evaporated off. The product, thus adsorbed on silica gel, was charged on the top of a column containing silica gel and was flushed with acetone to elute the mixture of cyclic oligomers. The product remained at the top of the column and was flushed with chloroform to separate the higher relative molecular mass part. The mixture of cyclic oligomers was separated into about 50 fractions by silica gel column chromatography with a mixture of acetone and hexanes (1:30 v/v). Each fraction was checked by TLC [developed by a mixture of acetone and hexanes (1:30 v/v) and detected with a UV lamp]. The fraction containing each cyclic oligomer was collected and the solvents were evaporated off on a rotary evaporator to produce the separated cyclic oligomer. The dimer and monomer were further purified by column chromatography with a mixture of acetone and hexanes (1:50 v/v). The cyclic oligomers were dissolved in chloroform, the solution was filtered, and oligomers were precipitated in methanol.

The same procedure as that used in the case of TPB-(*c*)-13(*z*) was used for the preparation and separation of TPB-(*c*)14(*z*) except that 1,14-dibromotetradecane was used instead of 1,13-dibromotridecane. The ratio of acetone and hexanes used for the separation by column chromatography was 1:50 v/v.

The same procedure as that used in the case of TPB-(*c*)13(*z*) oligomers was used for the preparation and separation of TPB-(*c*)18(*z*) except for the following conditions. TPB (0.637 g, 2.00 mmol), 1,18-dibromooctadecane (0.825 g, 2.00 mmol), TBAH (0.272 g, 0.800 mmol), *o*-dichlorobenzene (200 cm^3), and 10 mol dm^{-3} aq. NaOH (200 cm^3) were used. First, a mixture of chloroform and acetone (1:2 v/v) was used for the rough separation of cyclic oligomers from the high relative molecular mass part. A mixture of acetone and hexanes (1:50 v/v) was used for the fractionation of each cyclic oligomer. Only the cyclic monomer and dimer were obtained in relatively high purity.

The procedures used for the synthesis and separation of other macrocyclic oligomers based on TPB and α,ω-dibromoalkane containing *x* methylenic units [TPB-(*c*)*x*(*z*), *x* = 4–12] were almost identical with those described above and were reported in detail elsewhere.[3a-f]

Techniques.—1-D ^1H NMR (200 MHz) spectra were recorded on a Varian XL-200 NMR spectrometer. All spectra were acquired at room temperature with $SiMe_4$ as internal standard.

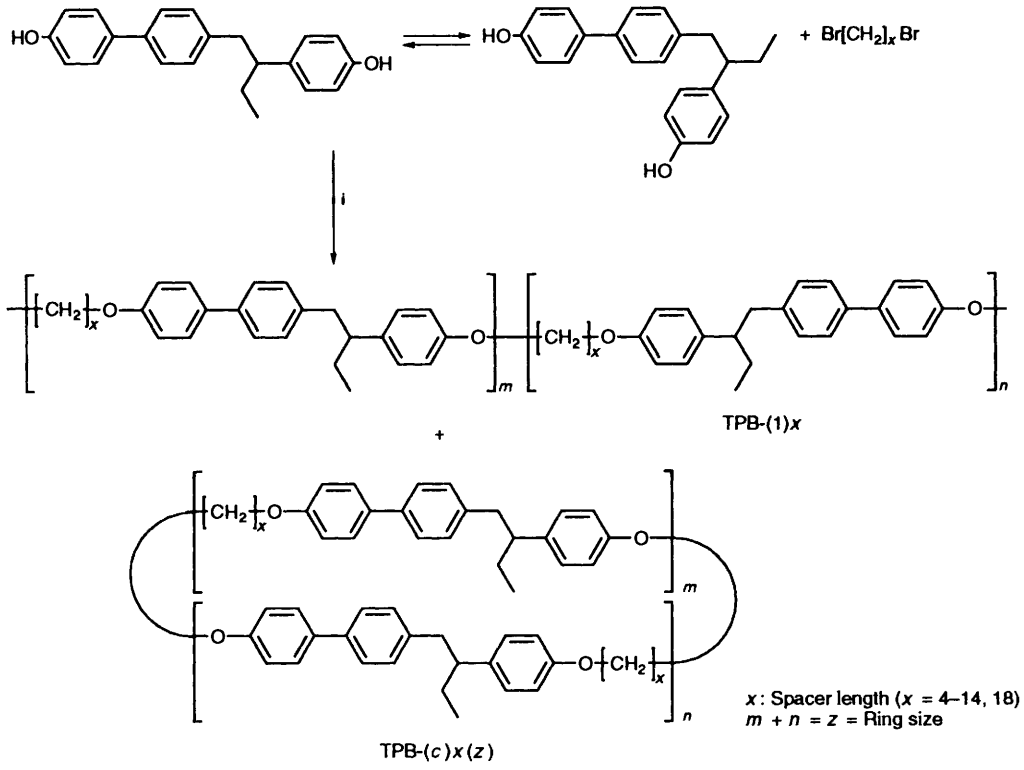

Scheme 1 Synthesis of cyclic polyethers [TPB-(*c*)*x*(*z*)] based on TPB and α,ω-dibromoalkanes containing *x* methylenic units *x* = 4–14, 18. *Reagents and conditions:* i, phase-transfer catalyst, *o*-dichlorobenzene, 10 mol dm^{-3} aq. NaOH (high dilution), 80 °C, 40 h.

Relative molecular masses and purities were determined by gel-permeation chromatography (GPC) and high-performance liquid chromatography (HPLC). GPC analyses were carried out with a Perkin-Elmer series 10 LC equipped with an LC-100 column oven, and a Nelson Analytical 900 series data station. The measurements were made by using the UV detector, chloroform as solvent (1 cm^3/min; 40 °C), two PL gel columns of gel size 5 × 10^2 and 10^4 Å, and a calibration plot constructed with polystyrene standards. HPLC analyses were performed with the same instrument with a PL gel column of 1 × 10^2 Å.

A Perkin-Elmer DSC-4 differential scanning calorimeter equipped with a TADS data station Model 3600 was used to determine thermal transitions. Heating and cooling rates were 20 °C/min in all cases. First-order transitions (crystalline–crystalline, crystalline–liquid crystalline, liquid crytalline–isotropic, *etc.*) were read at the maximum or minimum of the endothermic or exothermic peaks. Glass transition temperatures (T_g) were read at the middle of the change in the heat capacity. All heating and cooling scans after the first heating scan produced perfectly reproducible data. We will report the transitions collected from first and second or subsequent heating scans and from first cooling scan.

A Carl Zeiss optical polarizing microscope (magnification × 100) equipped with a Mettler FP 82 hot-stage and a Mettler FP 800 central processor was used to observe thermal transitions and to analyse anisotropic textures.

Results and Discussion

Cyclization of TPB with α,ω-Dibromoalkanes under High Dilution Conditions.—Scheme 1 outlines the synthesis of linear [TPB-(*l*)*x*] and cyclic [TPB-(*c*)*x*(*z*)] polyethers based on TPB and α,ω-dibromoalkanes containing *x* methylenic units. The influence of phase-transfer-catalysed polyetherification conditions (*i.e.*, monomer concentration, polymerization time) on the formation of cyclic and/or linear polyethers of TPB was discussed in a previous publication.[3a] Under high-dilution conditions, *i.e.*, 1 mmol TPB per 100 cm^3 of polymerization solvent, mostly cyclic low and high relative molar mass products were obtained. The mass fraction of each cyclic oligomer was estimated from the GPC chromatograms of the products obtained under high-dilution conditions and was plotted *versus* spacer length in Fig. 2. No cyclic monomer was formed with spacer lengths shorter than *x* = 6. This is due to the fact that this spacer is not long enough to form a cyclic structure with TPB. The mass fraction of cyclic monomer increases abruptly as the spacer length increases above *x* = 6 and becomes larger than that of cyclic dimers above *x* = 11. This sharp increase in the mass fraction of cyclic monomer is due to the fact that the ring strain decreases with the increase in spacer length. The mass fraction of dimers decreases with increasing spacer length with a slight odd–even effect which vanishes at longer spacer lengths. Odd spacers tend to yield a higher mass fraction of dimers compared with even spacers. This may be due to the more favourable conformation for the phenolate to attack the α carbon of the bromide group in the case of odd spacers. The mass fractions of trimers, tetramers, and pentamers including dimers decrease as the spacer length increases. This is simply due to the fact that the cyclic monomer is formed at the expense of higher oligomers.

Separation and Characterization of Cyclic Oligomers.—The low molar mass cyclic oligomers were separated from the linear and cyclic polymers by elution of the product with acetone on a silica gel column. The high relative molecular mass part was collected by elution with chloroform. The acetone-eluted fraction was used to separate the individual cyclic compounds by using a mixture of acetone and hexanes. Additional details are presented in the Experimental section. Figs. 3(*a*) and 3(*b*) present the GPC traces of the reaction mixture, of the high-relative molecular mass fraction eluted with $CHCl_3$, of the separated cyclic tetramer, trimer, dimer and monomer of TPB-(*c*)13(*z*), and the plot of the peak top molecular mass *versus* ring size, respectively. Figs. 4(*a*) and 4(*b*) present similar data for the

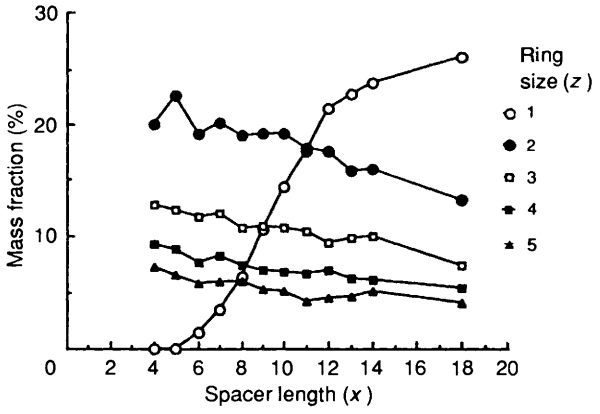

Fig. 2 Mass fractions of cyclic oligomers in the polymerization mixtures obtained from reactions performed under high-dilution conditions [monomer (mmol)/solvent (cm^3) 1/100] *versus* spacer length.

TPB-(*c*)14(*z*) series. Tables 1–3 summarize all the characterization results of the TPB-(*c*)13(*z*), TPB-(*c*)14(*z*), and TPB-(*c*)18(*z*) series. After column separation, cyclic oligomers from the dimer to tetramer with purities higher than 92% were obtained in both cases except for TPB-(*c*)14(4), whose purity was only 87% [Figs. 3(*a*) and 4(*a*), Tables 1–3]. The linear dependence of the peak top molecular mass *versus* the ring size demonstrates in both cases the correct assignment of the ring size [Figs. 3(*b*) and 4(*b*)].

The cyclic nature of these oligomers was demonstrated by 200 MHz 1-D ^1H NMR spectroscopy. Fig. 5 presents the assignment of the proton resonances of the linear polymer, of the high molecular mass part eluted with chloroform, and of the cyclic oligomers of TPB-(*c*)13(*z*) series, while Fig. 6 presents those of TPB-(*c*)14(*z*) series. These assignments agree with those of the cyclic TPB-(*c*)10(*z*) derivatives which were confirmed by extensive 2-D ^1H NMR-COSY and NOESY experiments.[3a] Two significant features of these spectra should be mentioned. First, these oligomers do not exhibit chain ends such as bromoalkane, phenol, olefin or alcohol.[3a] Secondly, the chemical shifts of methylene protons in the mesogenic unit (a, a'), methyl proton (d), and aromatic protons (A1–A6) are strongly dependent on ring size as shown in Fig. 7 for the case of the TPB-(*c*)13(*z*) series. Linear oligomers do not exhibit such a dependence. This behaviour is due to the change in the conformation of the TPB unit as a function of ring size which generates shielding and deshielding effects which were discussed in detail previously.[3a] If the chemical shifts of these protons are plotted *versus* spacer length instead of ring size, as for example in the case of the monomers TPB-(*c*)*x*(1), a similar dependence of the chemical shifts was observed (Fig. 8). It means that the increase in spacer length has a similar effect to that of an increase in ring size on the conformation of the TPB mesogenic unit, since as discussed in more detail in a previous paper,[3a] the chemical shifts of these protons are mainly determined by the conformation of TPB. This is quite reasonable since longer spacers allow the mesogen to adopt in the cyclic structure the conformation which is close to its *anti* conformer. However, it must be pointed out that even the cyclic monomer with the longest spacer prepared so far [*i.e.*, TPB-(*c*)18(1)] contains a high amount of *gauche* conformer in TPB since its aromatic protons are shifted significantly to upper fields [the chemical shifts of A4 and A5 protons which are the most sensitive protons to the conformation of TPB of TPB-(*c*)18(1) are at δ 6.84 and 6.80 respectively while those of linear TPB-(*l*)18 are at δ 7.08 and 7.04]. The dependence of the chemical shifts on spacer length decreases with increasing ring size as demonstrated in Fig. 9 for the tetramers TPB-(*c*)*x*(4) as an example.

Amplifications of the aliphatic region of the high relative molecular mass fractions separated from TPB-(*c*)13(*z*), TPB-(*c*)14(*z*), and TPB-(*c*)18(*z*) cyclization experiments show the presence of $-CH_2CH{=}CH_2$ (resonance at $\delta \sim 5.0$ for $=CH_2$) and CH_2OH ($\delta \sim 3.6$) chain ends which are formed, respectively, by elimination and by displacement of Br from $-CH_2Br$ by OH^-. Based on the integration results of these terminal groups *versus* those of the main chain groups in the NMR spectra and the number-average relative molecular masses obtained by GPC, it was calculated that ~67 mol% of the high relative molecular mass part which was separated from TPB-(*c*)13(*z*) series represents macrocyclics. On the other hand, the high relative molecular mass part of TPB-(*c*)14(*z*) and TPB-(*c*)18(*z*) series contains ~58 and 62 mol% respectively of macrocyclics. This is only an estimated value since the relative molecular masses measured by GPC are relative to polystyrene standards.

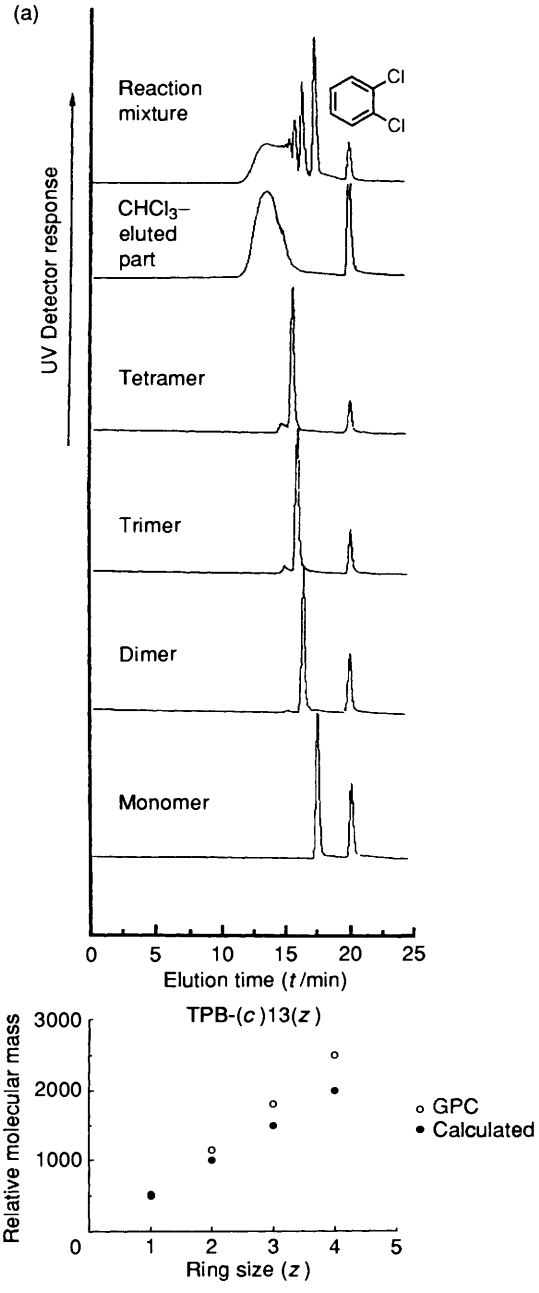

Fig. 3 (*a*) GPC chromatograms of the cyclization mixture, of the high relative molecular mass part, and of the separated cyclic oligomers [TPB-(*c*)13(*z*) series]; (*b*) the dependence of the peak molecular mass of cyclic oligomers TPB-(*c*)13(*z*) obtained by GPC (○), and calculated (●), *versus* ring size.

Table 1 Characterization of cyclic oligomers and corresponding linear polymer based on TPB and 1,13-dibromotridecane

Ring size (z)	Yield (%)	Purity by GPC (%)	Relative molecular mass by GPC at peak top: Measured	Calculated	Thermal transition (°C) and corresponding enthalpy changes (kcal/mru)[a] in parentheses[b]: Heating	Cooling
1	6.4	>9	518	499	k 96 (6.75) i g −4 i	i < −10 g
2	4.0	94.8	1146	997	g 67 k 90 (−0.55) 115 k 133 (6.84)[c] i k 109 k 129 (4.09)[c] i	i 91 (0.15) n 72 (3.27) k
3	2.3	93.3	1806	1496	g 31 s 58 (0.05) n 106 (0.69) i g 31 s 57 (0.06) n 106 (0.71) i	i 101 (0.66) n 52 (0.03) s 25 g
4	1.4	92.2	2499	1995	g 62 k 89 (2.24) n 115 (0.91) i g 34 k 48 (1.03) k 88 (1.65) n 115 (0.88) i	i 111 (0.98) n 37 (0.34) k 31 g
$CHCl_3$-eluted part	21.8	67[d]	M_n = 7.42 × 10^3 Mw/M_n = 1.78		g 39 k 45 (0.37) n 79 (1.20) i g 37 k 50 (0.20) n 79 (1.32) i	i 72 (1.24) n 41 (0.31) k 29 g
Linear			M_n = 3.29 × 10^4 Mw/M_n = 2.08		g 32 k 48 n 78 (2.47)[c] i g 41 k 47 (0.39) n 79 (1.48) i	i 70 (1.52) n 47 (0.38) k 32 g

[a] 1 cal = 4.184 J. [b] Data on the first line are from first heating and cooling scans. [c] Overlapped peaks. [d] Mol % of cyclic polymers.

Table 2 Characterization of cyclic oligomers and corresponding linear polymer based on TPB and 1,14-dibromotetradecane

Ring size (z)	Yield (%)	Purity by GPC (%)	Relative molecular mass by GPC at peak top: Measured	Calculated	Thermal transition (°C) and corresponding enthalpy changes (kcal/mru)[a] in parentheses[b]: Heating	Cooling
1	1.5	93.2	563	513	g 11 k 19 k 29 k 53 (−2.98)[c] k 98 (5.82) i g −5 i	i i < −10 g
2	1.3	95.7	1209	1026	k 95 k 106 k 121 (7.68)[c] i g 18 n 62 (−5.21) k 100 k 111 k 119	i 71 (0.25) n 12 g
3	2.0	98.3	1930	1538	(6.41)[c] i g 32 k 44 k 56 (0.77) s 70 (0.01) n 107	i 102 (0.76) n 65 (0.04) s 25 g
4	0.6	86.7	2590	2051	(0.71) i g 29 s 70 (0.02) n 107 (0.72) i	i 111 (0.98) n 37 (0.34) k 31 g
$CHCl_3$-eluted part	23.7	58[d]	M_n = 6.12 × 10^3 M_w/M_n = 1.67		g 62 k 89 (2.24) n 115 (0.91) i g 34 k 48 (1.03) k 88 (1.65) n 115 (0.88) i	i 89 (2.45) n 24 g
Linear			M_n = 3.02 × 10^4 M_w/M_n = 2.16		g 36 k 48 (0.43) k 75 n 85 (4.53)[c] i g 41 k 74 n 84 (4.36)[c] i g 38 k 58 (0.26) k 64 (−0.34) k 84 n 96 (3.97)[c] i g 49 k 85 (1.83) n 96 (2.57) i	i 83 (2.71) n 60 (1.85) k 43 g

[a–d] See footnotes in Table 1.

Table 3 Characterization of cyclic oligomers and corresponding linear polymer based on TPB and 1,18-dibromooctadecane

Ring size (z)	Yield (%)	Purity by GPC (%)	Relative molecular mass by GPC at peak top: Measured	Calculated	Thermal transition (°C) and corresponding enthalpy changes (kcal/mru)[a] in parentheses[b]: Heating	Cooling
1	20.0	>99	646	569	k 64 (10.52) i g −3 i	i −11 g
2	1.87	91.5	1371	1138	g 54 k 102 k 111 (9.97)[c] i k 59 (−0.98) k 112 k 118 (8.61)[c] i	i 78 (0.36) n 44 k 35 (5.22)[c] k
$CHCl_3$-eluted part	20.9	62[d]	M_n = 5.77 × 10^3 M_w/M_n = 1.80		g 39 (−0.97) k 84 (5.40) i g 43 k 84 (5.89) i	i 69 (5.36) k 28 g
Linear			M_n = 3.71 × 10^4 M_w/M_n = 3.88		g 34 k 65 k 91 (3.56)[c] i g 37 n 91 (5.81) i	i 72 (5.61) n 35 g

[a–d] See footnotes in Table 1.

Mesomorphic Behaviour of TPB-(c)13(z), *TPB-*(c)14(z), *and TPB-*(c)18(z).—The differential scanning calorimetry (DSC) traces of the individual macrocyclics, of the high relative molecular mass macrocyclics and of the high relative molecular mass linear polymers of the TPB-(*c*)13(*z*), TPB-(*c*)14(*z*), and TPB-(*c*)18(*z*) series are presented in Figs. 10–12, respectively. The characterization data are summarized in Tables 1–3 where they are also compared with the phase behaviour of their linear homologues.

On its first heating scan TPB-(*c*)13(1) is crystalline. However, on subsequent heating and cooling scans it displays only a glass transition. TPB-(*c*)13(2) exhibits, regardless of its thermal history, only a crystalline melting during heating scans. However, it displays a small peak before crystallization on cooling, which is most probably the isotropic–nematic transition. TPB-(*c*)13(3) displays an enantiotropic nematic mesophase followed by a smectic phase which was characterized by X-ray diffraction experiments. The nematic–smectic transition

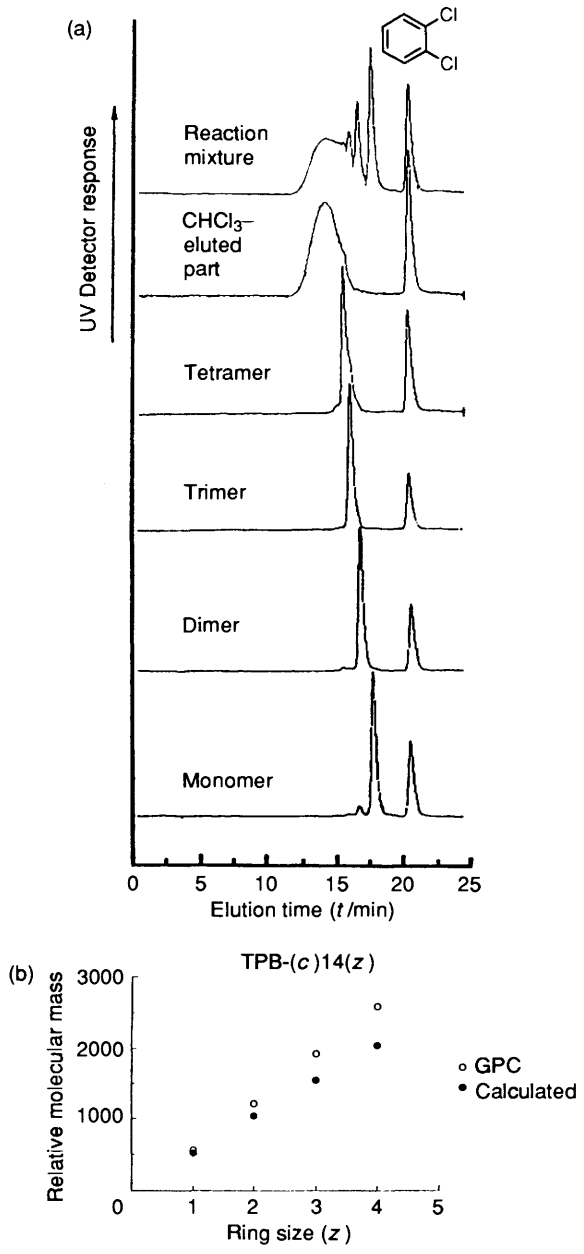

Fig. 4 (*a*) GPC chromatograms of the cyclization mixture, of the high relative molecular mass part, and of the separated cyclic oligomers [TPB-(*c*)14(*z*) series]; (*b*) the dependence of the peak molecular mass of cyclic oligomers TPB-(*c*)14(*z*) obtained by GPC (○), and calculated (●), *versus* ring size.

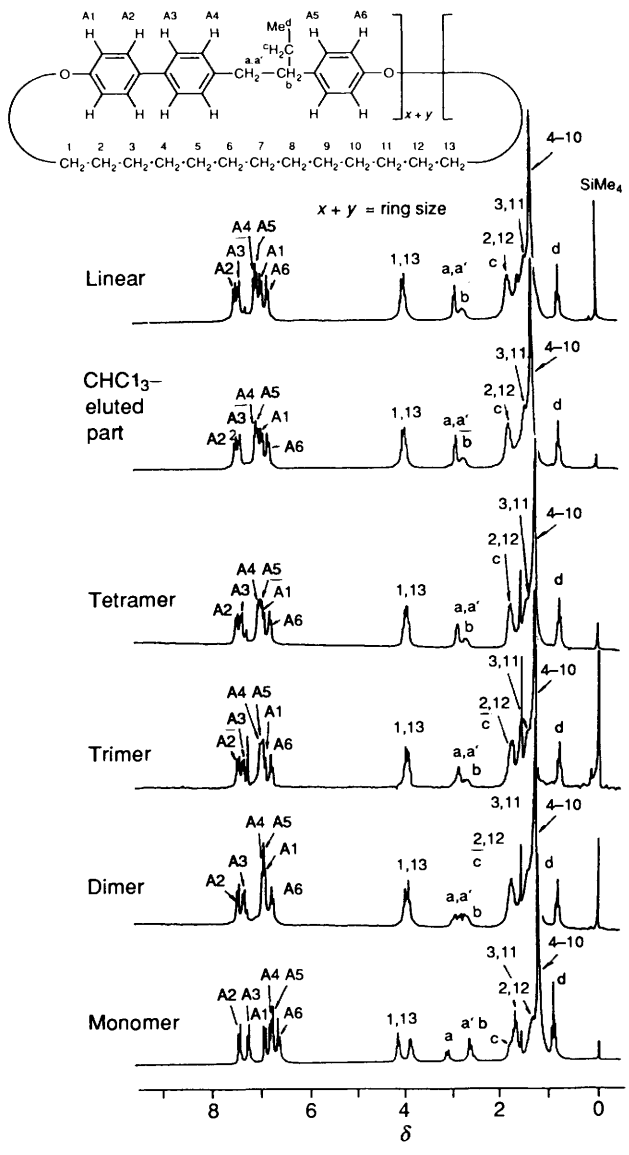

Fig. 5 The 200 MHz ^{1}H NMR spectra ($CDCl_3$; $SiMe_4$), and the corresponding protonic assignments of the cyclic oligomers, of the $CHCl_3$-eluted part of the TPB-(*c*)13(*z*) series, and of the linear polymer TPB-(*l*)13.

peak is very small as seen in Fig. 10. However, the texture change is rather drastic as presented in Fig. 13. The complete characterization of this smectic phase by X-ray diffraction experiments will be reported elsewhere.[18] TPB-(*c*)13(4) displays multiple crystalline phases and an enantiotropic nematic phase. Representative textures of the nematic phase of TPB-(*c*)13(4) are presented in Fig. 14. The nematic–isotropic transition temperatures and their associated enthalpy changes increase with increasing ring size. TPB-(*c*)13(3) and TPB-(*c*)13(4) display higher isotropization temperatures. However, their associated enthalpy and entropy changes are lower than those of their linear high relative molecular mass homologues. The high relative molecular mass fraction of TPB-(*c*)13(*z*) displays similar phase behaviour to that of the linear polymer TPB-(*l*)13.

The phase behaviour of TPB-(*c*)14(*z*) and TPB-(*l*)14 will be discussed by following Fig. 10 and Table 2. TPB-(*c*)14(1) displays similar phase behaviour to that of TPB-(*c*)13(1), *i.e.*, it is crystalline during the first DSC heating scan and subsequently it remains glassy. TPB-(*c*)14(2) displays a monotropic nematic mesophase. While during the first heating scan it is only crystalline, during the second heating scan TPB-(*c*)14(2) crystallizes above the nematic–isotropic transition temperature. TPB-(*c*)14(3) displays identical behaviour with that of TPB-(*c*)13(3), *i.e.*, it exhibits enantiotropic nematic and smectic mesophases and it does not crystallize regardless of its thermal history. TPB-(*c*)14(4) displays an enantiotropic nematic mesophase and a crystalline phase both during heating and cooling scans. The nematic–isotropic transition peak was rather broad in this case. This may be due to the relatively low purity of the sample (87% by HPLC). TPB-(*c*)14(3) and TPB-(*c*)14(4) exhibit higher isotropization temperatures although their associated enthalpy and entropy changes are lower than those of their linear high relative molecular mass homologue. The high relative molecular mass fraction of TPB-(*c*)14(*z*) displays similar phase behaviour to that of the linear polymer TPB-(*l*)14 except that the peaks are much broader than those exhibited by the linear polymers.

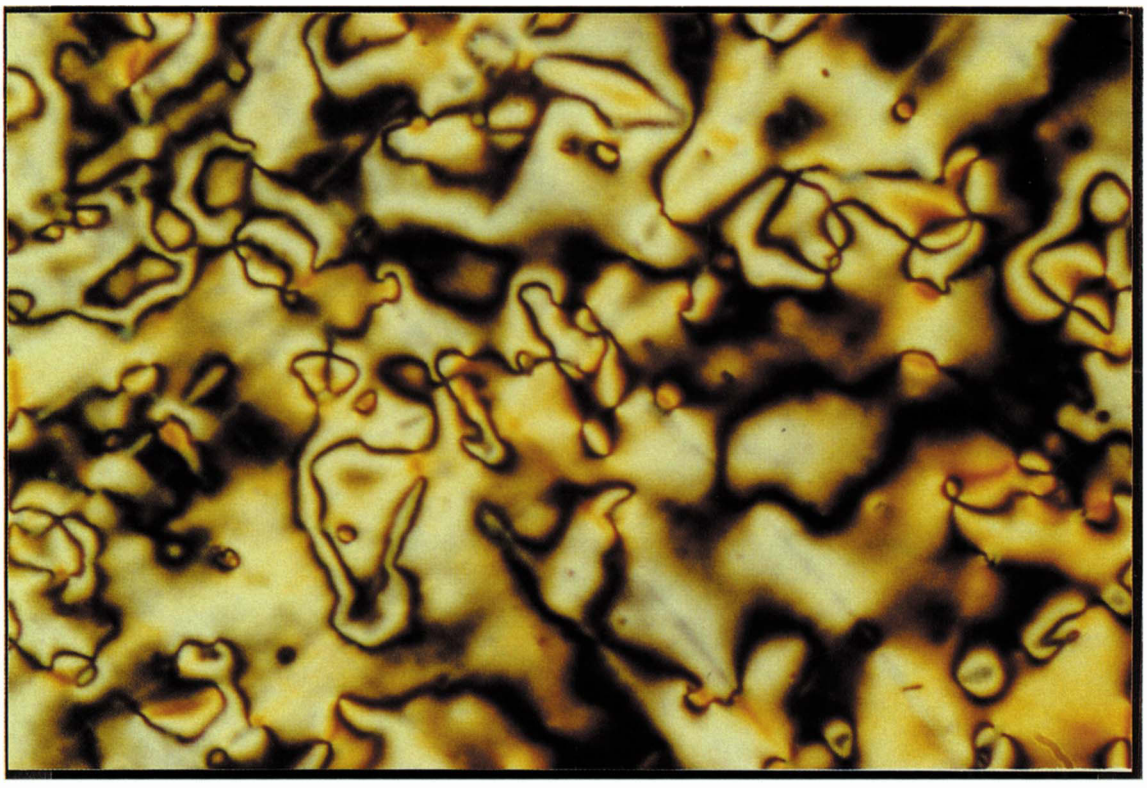

(*b*)

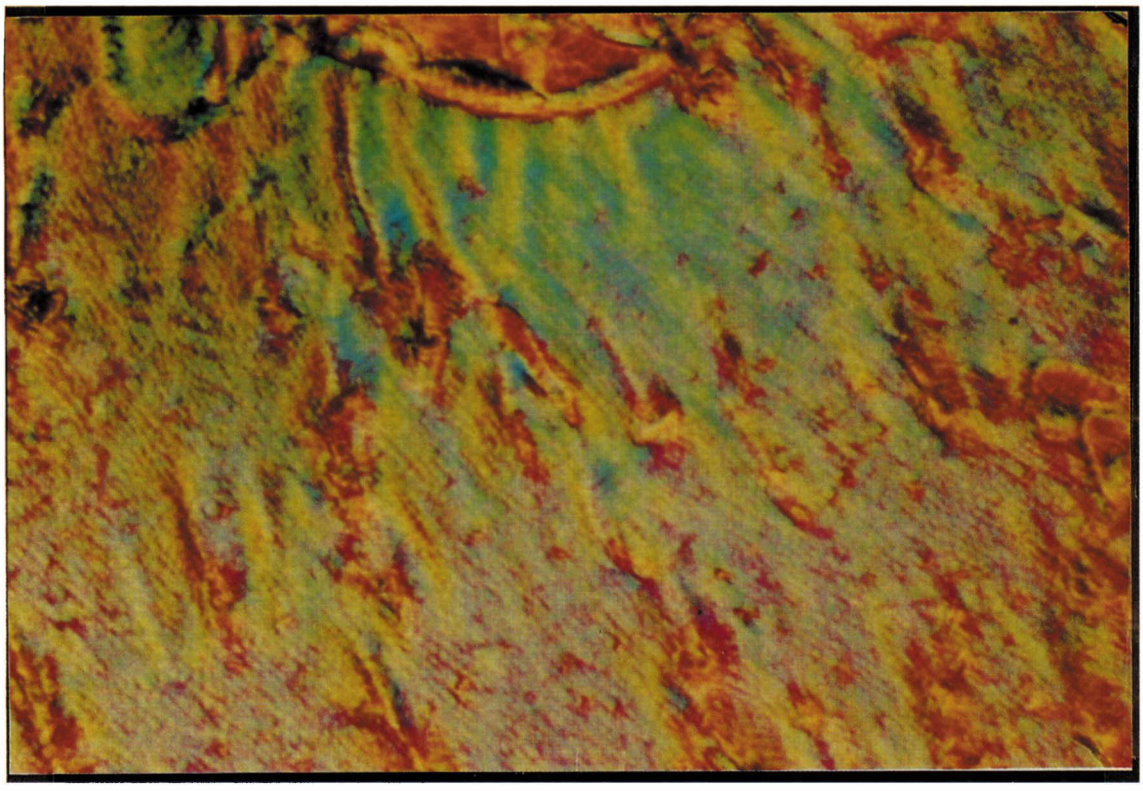

[Facing p. 1324]

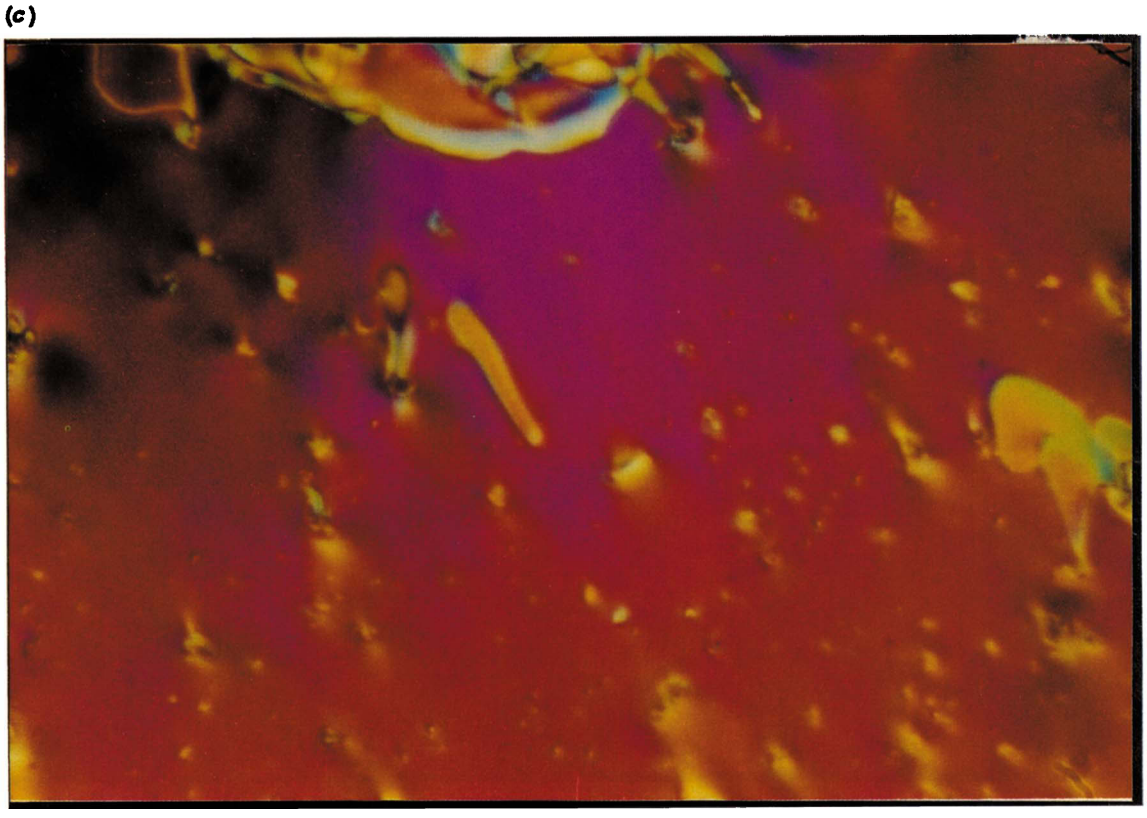

Fig. 13 Representative optical polarized micrographs (× 100) of (a) the nematic phase of TPB-(*c*)13(4) (after annealing at 95 °C for 2 min); (b) the smectic phase of TPB -(*c*)13(3) (after annealing at 45 °C for 5 min); (c) the nematic phase of TPB-(*c*)13(3) [heated up from (b) to 60 °C].

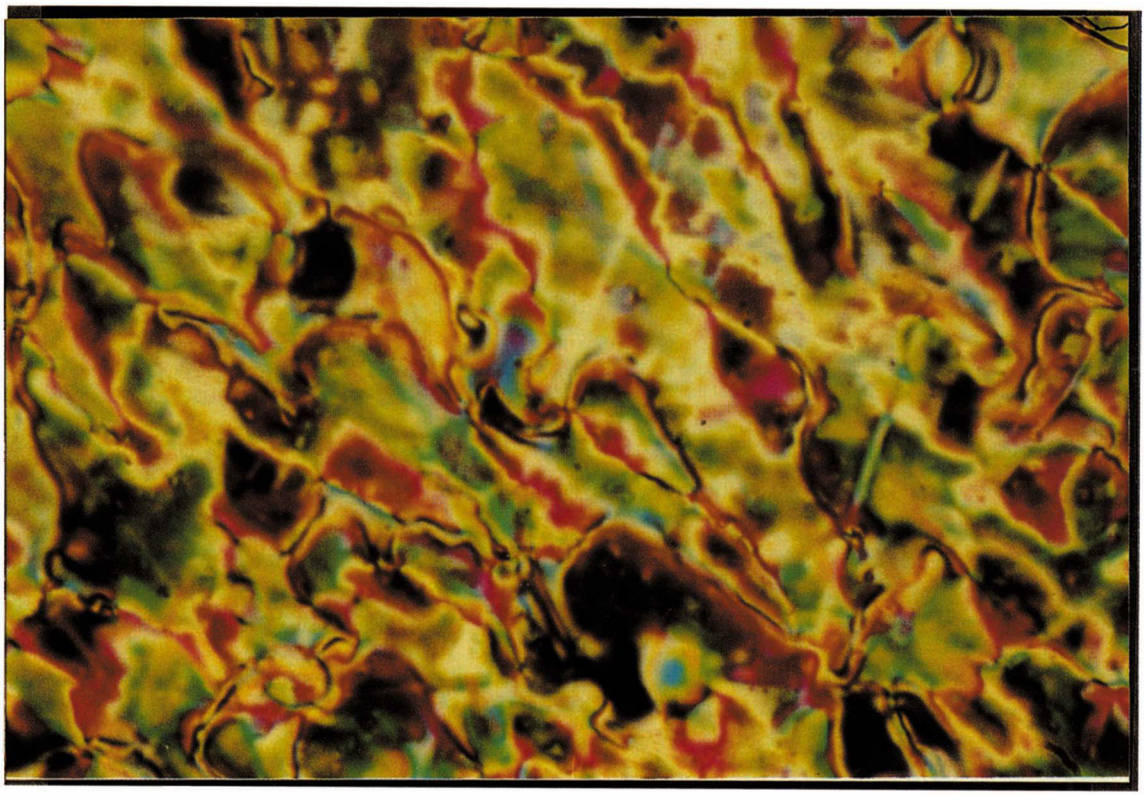

Fig. 14 Representative optical polarized micrograph (× 100) of the nematic phase of TPB-(*c*)13(4) after annealing at 95 °C for 1.5 min.

Table 4 Characterization of cyclic monomers [TPB-(*c*)*x*(1)] based on TPB and α,ω-dibromoalkanes containing *x* methylenic units

Spacer length (*x*)	Purity (HPLC) (%)	Thermal transitions (°C) and corresponding enthalpy changes (kcal/mru)[a] in parentheses[b]	
		Heating	Cooling
9	98	liquid	liquid
10	99	g −10 i g −10 i	i −10 g
11	>99	k 88 (6.24) i g −4 i	i −11 g
12	>99	k 102 (8.31) i g −7 i	i −10 g
13	>99	k 96 (6.75) i g −4 i	i −10 g
14	93	g 11 k 19 k 29 k 53 (−2.98)[c] k 98 (5.82) i g −5 i	i −10 g
18	>99	k 64 (10.52) i g −3 i	i −11 g

[a]–[c] See footnotes in Table 1.

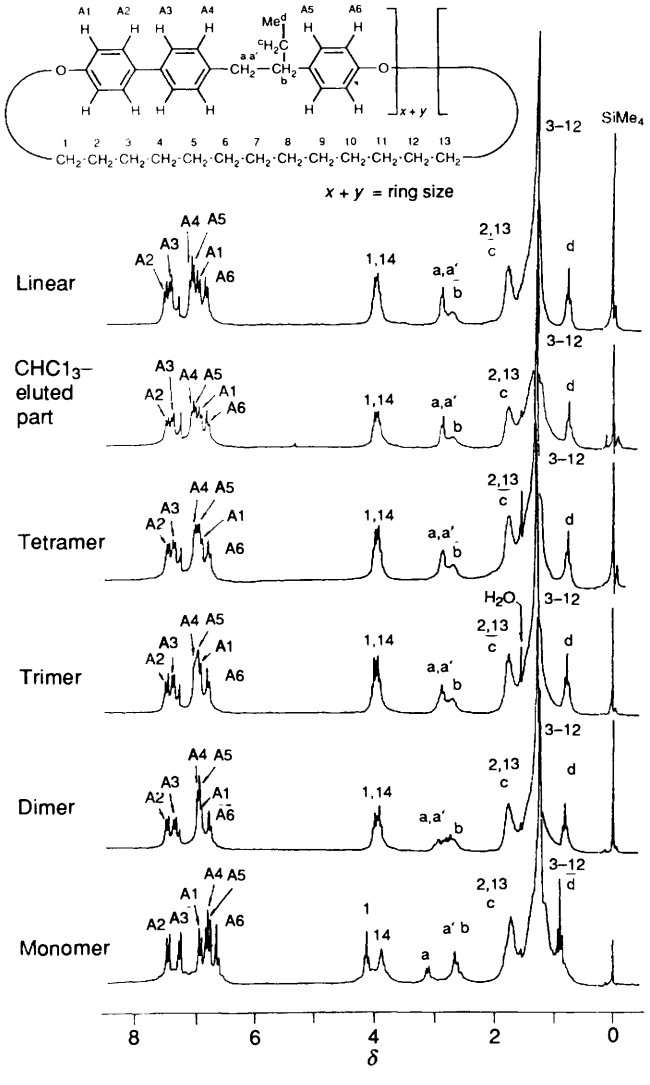

Fig. 6 The 200 MHz ^{1}H NMR spectra ($CDCl_3$; $SiMe_4$), and the corresponding protonic assignments of the cyclic oligomers, of the $CHCl_3$-eluted part of the TPB-(*c*)14(*z*) series, and of the linear polymer TPB-(*l*)14.

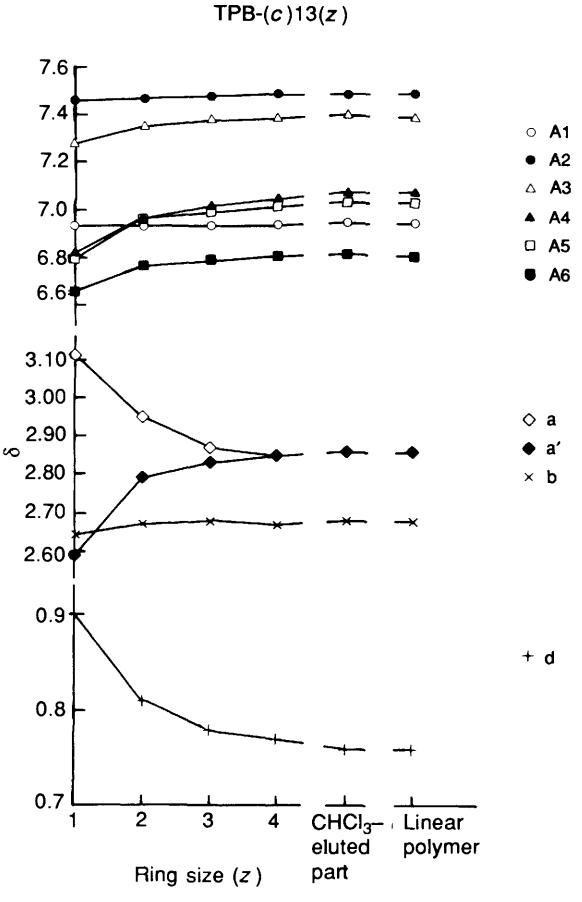

Fig. 7 The dependence of the chemical shifts of the most representative protonic resonances of TPB-(*c*)13(*z*) cyclics as a function of ring size and their comparison with that of the linear polymer.

There are only very few data on the TPB-(*c*)18(*z*) series. TPB-(*c*)18(1) is crystalline during the first DSC heating scan and on subsequent DSC scans it remains glassy. TPB-(*c*)18(2) displays only a crystalline phase during first and subsequent heating scans. A monotropic nematic mesophase was observed during the cooling scan of TPB-(*c*)18(2).

General Trend of the Mesomorphic Behaviour of Cyclic Oligomers.—Tables 4–6–8–10 summarize all the phase transitions of TPB-(*c*)*x*(*z*) series with *x* = 4–14, and 18 for the monomer (*z* = 1), dimer (*z* = 2), trimer (*z* = 3), tetramer (*z* = 4), pentamer (*z* = 5), and of the high relative molecular mass cyclic fraction. The detailed synthesis and characterization of macrocyclics TPB-(*c*)*x*(*z*) with *x* = 4,6,[3d] 5,[3b] 7,[3c] 8,9,[3e] 10[3a] and 11, 12[3f] were described elsewhere.

General Trend of Cyclic Monomers.—Table 4 summarizes all

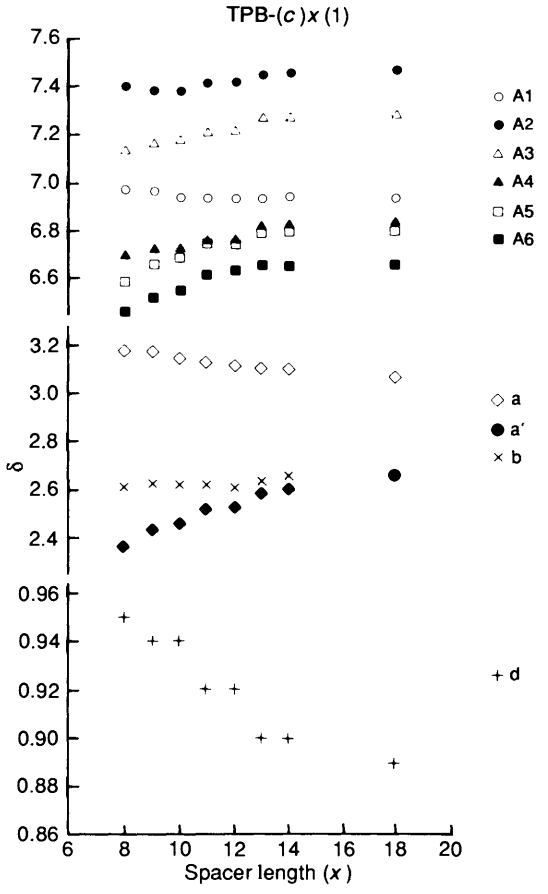

Fig. 8 The dependence of chemical shifts of: aromatic protons (A1–A6), the protons of the lateral ethyl group (c and d), methylenic protons next to the biphenyl ring (a and a') and methine proton (b) *versus* spacer length (x) for the cyclic monomers [TPB-(c)x(1)].

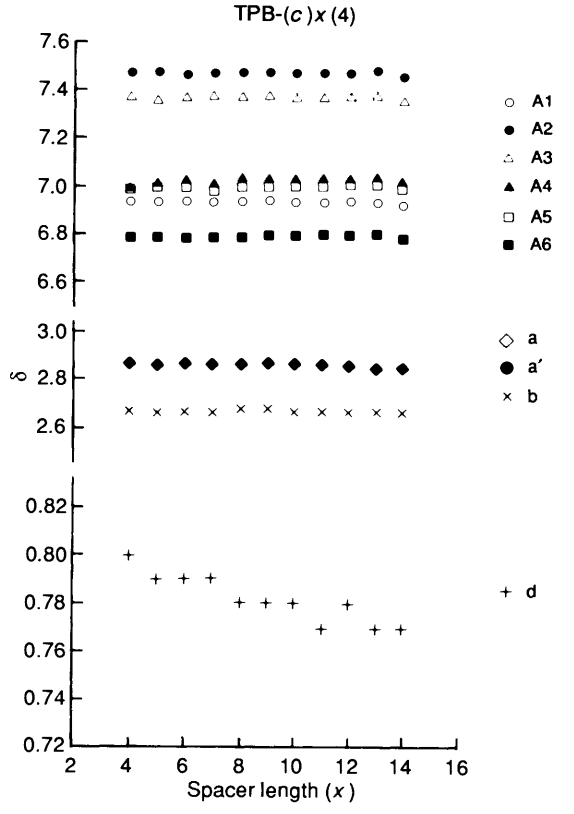

Fig. 9 The dependence of chemical shifts of: aromatic protons (A1–A6), the protons of the lateral ethyl group (c and d), methylenic protons next to the biphenyl ring (a and a') and methine proton (b) *versus* spacer length (x) for the cyclic tetramers [TPB-(c)x(4)].

the data of the cyclic monomers, TPB-(c)x(1). As seen from Table 4, all cyclic monomers synthesized are liquid or crystalline compounds during their first heating cycle. However, they do not crystallize on subsequent cooling and heating scans. No mesophase was observed for any of these cyclic monomers. This is quite reasonable since as discussed in the NMR part the cyclic monomers have the conformation of the TPB mesogenic unit close to that of the *gauche* conformer. The TPB unit with such a conformation is no longer a rod-like molecule and cannot generate a liquid crystalline phase regardless of whether it is part of a linear or part of a cyclic structure.

General Trend of Cyclic Dimers.—Table 5 summarizes all the data of the cyclic dimers, TPB-(c)x(2). Fig. 15a–c presents the phase-transition temperatures *versus* spacer length (x) obtained from the first heating, second heating, and cooling scans of the dimers. The general trend displayed by these dimers can be summarized as follows. Most of the dimers exhibit several melting peaks on their first heating scan. The m.p. decreases with increasing spacer length. Some of the dimers with spacer length longer than $x = 9$ exhibit a monotropic nematic mesophase, *i.e.*, one that is observed only during cooling scans. The dimers with the spacer length shorter than $x = 9$ do not display any mesophase. This behaviour can be explained as follows. First, these dimers display a higher crystallization tendency and, therefore, crystallize at a relatively higher temperature during cooling scans than that at which the expected virtual isotropic–nematic transition should occur. Secondly, as expected from the opposite trends exhibited by

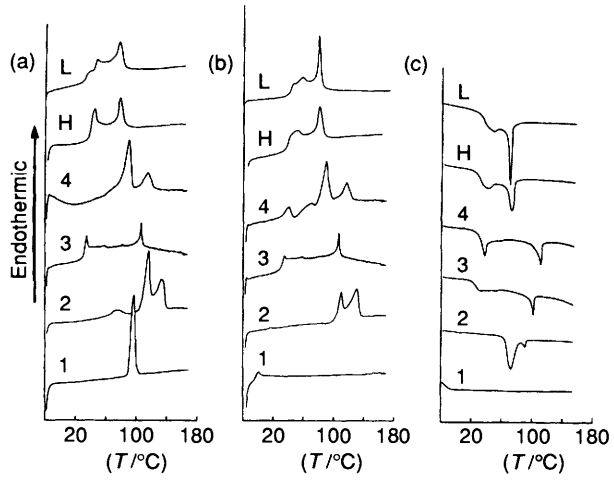

Fig. 10 Representative DSC traces (20 °C/min) of: (a) first heating; (b) second heating; and (c) first cooling scans of cyclic oligomers [TPB-(c)13(z); the numbers in the Figure indicate the ring rize (z)], of the $CHCl_3$-eluted part [TPB-(c)13, indicated as H], and of the linear polymer [TPB-(l)13, indicated as L].

the isotropic–nematic transition temperatures (T_{in}) and glass transition temperature (T_g) *versus* spacer length, T_{in} becomes lower than T_g for spacer length shorter than $x = 8$ and the formation of mesophane is kinetically prohibited (Fig. 15c). The isotropic–nematic transitions of the dimers with even spacers increase with increasing spacer length. There is only one data point of the dimer with the odd spacer $x = 13$. Although the trend is not clear, since TPB-(c)13(2) exhibits a higher transition temperature than that of the dimers with even spacers, the T_{in} transition temperature of the dimers may show an inverse odd–

Table 5 Characterization of cyclic dimers [TPB-(*c*)*x*(2)] based on TPB and α,ω-dibromoalkanes containing *x* methylenic units

Spacer length (*x*)	Purity (HPLC) (%)	Thermal transitions (°C) and corresponding enthalpy changes (kcal/mru)[a] in parentheses[b] Heating	Cooling
4	99	k 181 (2.24) i g 62 i	i 58 g
5	97	k 163 (−1.36) k 179 k 183 (5.79)[c] i g 61 k 104 (−2.28) k 173 (4.23) i	i 103 (0.78) k 55 g
6	>99	k 196 (8.94) i g 55 k 101 (−1.01) k 158 (−2.67) k 192 k 197 k 203 (8.34)[c] i	i 105 (2.86) k 49 g
7	>99	k 171 k 180 (6.84)[c] i k 150 (−0.99) k 166 k 172 k 180 (5.53)[c] i	i 111 (4.01) k
8	98	k 127 k 139 k 145 (6.30)[c] i g 37 i 90 k 121 (−4.58) k 142 k 147 (4.41) i	i 31 g
9	98	g 42 k 134 (4.61) i k 97 (−0.54) k 117 k 121 (2.17) k 134 (1.62) i	i 80 (2.75) k
10	92	g 53 k 90 k 113 (5.78)[c] i g 23 n 46 (0.15) i	i 41 (0.08) n 17 g
11	>99	k 110 k 132 (6.81)[c] k 144 (0.64) i k 112 k 132 (4.63)[c] i	i 94 (3.94) k
12	97	k 110 k 130 (7.40)[c] i g 16 n 61 (0.22) i 75 (−0.30) k 111 (0.30) i	i 56 (0.21) n 10 g
13	95	g 67 k 90 (−0.55) 115 k 133 (6.84)[c] i k 109 k 129 (4.09)[c] i	i 91 (0.15) n 72 (3.27) k
14	96	k 95 k 106 k 121 (7.68)[c] i g 18 n 62 (−5.21) k 100 k 111 k 119 (6.41)[c] i	i 71 (0.25) n 12 g
18	92	g 54 k 102 k 111 (9.97)[c] i k 59 (−0.98) k 112 k 118 (8.61)[c] i	i 78 (0.36) n 44 k 35 (5.22)[c] k

[a]–[d] See footnotes in Table 1.

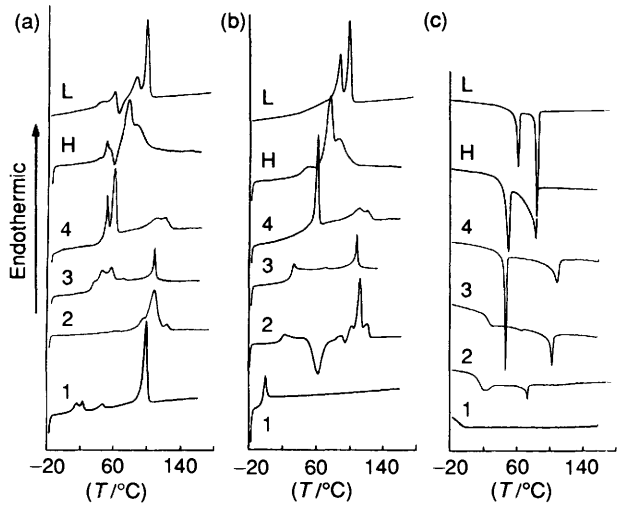

Fig. 11 Representative DSC traces (20 °C/min) of: (a) first heating; (b) second heating; and (c) first cooling scans of cyclic oligomers [TPB-(*c*)14(*z*); the numbers in the Figure indicate the ring size (*z*)], of the $CHCl_3$-eluted part [TPB-(*c*)14, indicated as H], and of the linear polymer [TPB-(*l*)14, indicated as L].

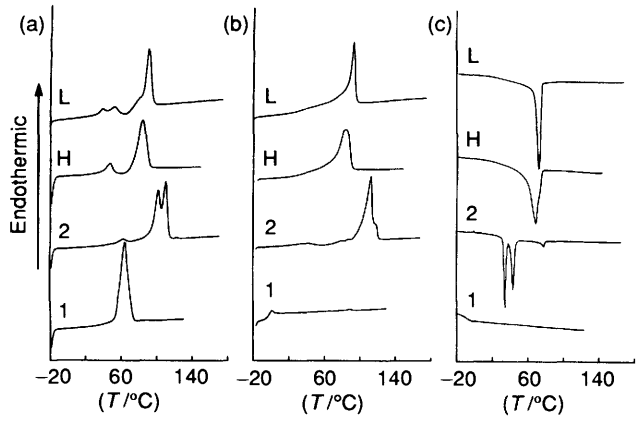

Fig. 12 Representative DSC traces (20 °C/min) of: (a) first heating; (b) second heating; and (c) first cooling scans of cyclic oligomers [TPB-(*c*)18(*z*); the numbers in the Figure indicate the ring size (*z*)], of the $CHCl_3$-eluted part [TPB-(*c*)18, indicated as H], and of the linear polymer [TPB-(*l*)18, indicated as L].

even effect compared with the odd–even effect of linear TPB-X polymers which was discussed in a previous paper.[4] The glass transition temperature of these dimers decreases with increasing spacer length as in the case of the linear homologous polymers. During the second heating scan, most of the dimers exhibit glass and crystallization transitions followed by melting. TPB-(*c*)10(2) and TPB-(*c*)12(2) exhibited a nematic mesophase since these dimers did not crystallize on their cooling scan.

General Trend of Cyclic Trimers.—Table 6 summarizes all the data of the cyclic trimers, TPB-(*c*)*x*(3). Fig. 16a presents the phase-transition temperatures obtained from the first heating scan, while Fig. 16b presents their phase-transition temperatures obtained from the second heating and cooling scans of the species TPB-(*c*)*x*(3). Most of the trimers exhibit a nematic phase with very little tendency toward crystallization. Even on the first heating scan, only TPB-(*c*)4(3), TPB-(*c*)6(3), and TPB-(*c*)10(3) exhibit a melting transition peak. During cooling and second heating scans, none of the trimers exhibit crystallization or melting transitions. TPB-(*c*)4(3) exhibits only a glass transition during first cooling and second heating scans. TPB-(*c*)6(3) shows a transition to a monotropic mesophase during cooling and second heating scans. This phase was difficult to identify since the texture obtained on the optical polarized microscope is very fine and upon annealing it crystallizes. However, this may also be a higher order mesophase since the enthalpy change of this transition is much higher than the value expected from the trend presented in Fig. 17. The nematic–isotropic transition temperature increases as the spacer length increases with an opposite odd–even effect to that of the linear TPB-(*l*)*x* series (Fig. 16a, b). Also, the enthalpy change associated with the nematic–isotropic transition increases

Table 6 Characterization of cyclic trimers [TPB-(*c*)*x*(3)] based on TPB and α,ω-dibromoalkanes containing *x* methylenic units

Spacer length (*x*)	Purity (HPLC) (%)	Thermal transitions (°C) and corresponding enthalpy changes (kcal/mru)[a] in parentheses[b]	
		Heating	Cooling
4	97	k 140 (2.12) k 152 (−1.44) 176 (1.36) i g 70 i	i 64 g
5	95	g 60 k 68 (0.26) i g 63 i	i 59 g
6	95	k 132 k 148 (3.46)[c] i g 63 s 80 (0.35) i	i 74 (0.37) s 59 g
7	92	g 52 n 81 (0.07) i g 49 n 81 (0.08) i	i 77 (0.07) n 46 g
8	92	g 43 s 69 (0.15) n 83 (0.08) i g 43 s 69 (0.15) n 83 (0.08) i	i 79 (0.07) n 66 (0.15) s 37 g
9	95	g 43 n 96 (0.19) i g 40 n 96 (0.19) i	i 92 (0.18) n 36 g
10	95	g 37 k 63 (1.19) n 95 (0.27) i g 28 n 94 (0.32) i	i 87 (0.32) n 20 g
11	91	g 35 n 105 (0.56) i g 33 n 104 (0.48) i	i 98 (0.49) n 26 g
12	95	g 27 n 103 (0.62) i g 27 n 103 (0.62) i	i 98 (0.63) n 22 g
13	93	g 31 s 58 (0.05) n 106 (0.69) i g 31 s 57 (0.06) n 106 (0.71) i	i 101 (0.66) n 52 (0.03) s 25 g
14	98	g 32 k 44 k 56 (0.77) s 70 (0.01) n 107 (0.71) i g 29 s 70 (0.02) n 107 (0.72) i	i 102 (0.76) n 65 (0.04) s 25 g

[a] [c] See footnotes in Table 1.

Table 7 The length of TPB unit, spacers, and of fully extended TPB-*x* monomer unit

The number of methylenic units (*x*)	The length of spacer[a] (Å)	The total length of fully extended monomer unit[a] (Å)
4	6.1	22.2
5	7.4	23.5
6	8.6	24.7
7	9.9	26.0
8	11.1	27.2
9	12.4	28.5
10	13.6	29.7
11	14.9	31.0
12	16.1	32.2
13	17.4	33.5
14	18.6	32.7
15	19.9	39.0
16	21.1	37.2
17	22.4	38.5
18	23.6	39.7

[a] The length measured from oxygen to oxygen by Alchemy II. The length of the TPB unit was 16.1 Å in all cases.

drastically with increasing spacer length (Fig. 17). No odd–even effect accompanies the dependence of this enthalpy change on spacer length. This can be explained as follows. From the X-ray and molecular modelling results,[5] in the nematic phase, the *anti* conformer of the TPB mesogenic unit is the dominant species and it is aligned parallel to another TPB unit. Therefore, the ideal conformation of the trimer in the nematic state should contain the *anti* conformer of the mesogenic unit which is fully aligned in one direction as shown in Scheme 2. The length of the TPB mesogenic unit and that of spacers obtained by computer modelling are listed in Table 7. The minimum length of the spacer required to generate an ideal conformation for the liquid crystalline trimer was roughly estimated by eqn. (1) which assumes that, at its minimum length, the length of the sum of

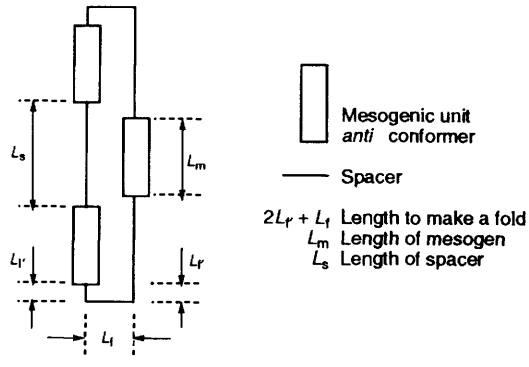

Scheme 2 Schematic representation of the ideal conformation of cyclic trimers in the nematic state.

$$2L_m + L_s = 2(L_s - 2.5) + L_m \quad (1)$$

two mesogens and one extended spacer should be equal to the sum of the lengths of one mesogen and of the remaining parts of the two spacers which do not contribute to the fold. The rest of the spacer is needed to make a fold. The minimum number of carbons of one spacer to achieve the 180° turn in the fold is two or more, namely 2.5 Å or longer. However, we assume here that it is only 2.5 Å (Scheme 2).

In eqn. (1) L_m is the length of the mesogen while L_s is the length of the spacer (Scheme 2). From eqn. (1) and the length of mesogen from Table 7, the minimum length of the spacer for the ideal conformation of the trimer is 21 Å. Therefore, the ideal conformation is almost impossible in a cyclic trimer before the spacer length is longer than $x = 15$ (Table 7). The cyclic trimers with spacer length shorter than $x = 15$ should have a distorted conformation compared with the ideal one. This distortion of the conformation of the trimers decreases the strong odd–even dependence of the transition temperature and of its associated enthalpy change. On the other hand, the extent of distortion should be dependent on the spacer length. Namely, as the spacer length increases the conformation of the trimer should

Table 8 Characterization of cyclic tetramers [TPB-(*c*)*x*(4)] based on TPB and α,ω-dibromoalkanes containing *x* methylenic units

Spacer length (*x*)	Purity (HPLC) (%)	Thermal transitions (°C) and corresponding enthalpy changes (kcal/mru)[a] in parentheses[b]	
		Heating	Cooling
4	96	g 59 k 123 (−1.85) k 188 (1.75) i g 60 n 114 (0.23) i	i 109 (0.31) n 55 g
5	94	g 66 k 73 k 80 (0.37)[c] n 103 (0.08) i g 64 n 103 (0.11) i	i 100 (0.12) n 60 g
6	96	g 55 k 75 (0.13) n 148 (0.90) i g 61 n 149 (0.79) i	i 145 (0.85) n 54 g
7	93	g 52 k 64 (0.12) n 115 (0.28) i g 50 n 114 (0.34) i	i 111 (0.29) n 46 g
8	95	g 18 k 75 (0.41) n 132 (1.06) i g 36 n 141 (0.95) i	i 133 (0.84) n 31 g
9	94	g 41 n 121 (0.47) i g 40 n 121 (0.48) i	i 118 (0.42) n 37 g
10	96	g 50 k 55 k 82 k 121 n 130 (3.13)[c] i g 29 n 127 (1.21) i	i 124 (1.18) n 25 g
11	92	g 38 k 59 (−1.20) k 81 (0.52) k 103 n 116 (1.77)[c] i g 34 n 67 (−0.76) k 83 (0.55) n 116 (0.71) i	i 112 (0.73) n 27 g
12	95	g 44 n 66 k 89 (−2.51)[a] 115 n 124 (3.89)[c] i g 29 n 54 k 82 (−2.29)[c] k 115 n 125 (3.78)[c] i	i 121 (1.38) n 23 g
13	92	g 62 k 89 (2.24) n 115 (0.91) i g 34 k 48 (1.03) k 88 (1.65) n 115 (0.88) i	i 111 (0.98) n 37 (0.34) k 31 g
14	87	g 62 k 89 (2.24) n 115 (0.91) i g 34 k 48 (1.03) k 88 (1.65) n 115 (0.88) i	i 111 (0.98) n 37 (0.34) k 31 g

[a] [c] See footnotes in Table 1.

Table 9 Characterization of cyclic pentamers [TPB-(*c*)*x*(5)] based on TPB and α,ω-dibromoalkanes containing *x* methylenic units

Spacer length (*x*)	Purity (HPLC) (%)	Thermal transitions (°C) and corresponding enthalpy changes (kcal/mru)[a] in parentheses[b]	
		Heating	Cooling
5	92	g 64 k 68 (0.10) k 80 (0.30) n 94 (0.07) i g 63 n 93 (0.10) i	i 89 (0.12) n 59 g
7	89	g 47 n 108 (0.29) i g 51 n 107 (0.36) i	i 103 (0.27) n 48 g
8	77	g 42 n 123 (1.01) i g 38 n 128 (1.00) i	i 128 (0.65) n 33 g
9	91	g 46 n 110 (0.32) i g 44 n 110 (0.35) i	i 107 (0.52) n 42 g
10	*d*	g 36 k 45 (0.09) n 127 (1.21) i g 33 n 128 (1.14) i	i 123 (1.19) n 26 g
11	91	g 39 n 108 (0.76) i g 35 X 47 (0.02) n 109 (0.81) i	i 105 (0.89) n 39 (0.06) X 31 g

[a] [c] See footnotes in Table 1. [d] It contains trimer, tetramer, and higher cyclics. However, each cyclic is overlapped severely and purity could not be determined.

approach the ideal one. Naturally, the transition temperature and the enthalpy change associated with this transition should increase with increasing spacer length. Although the opposite odd–even effect cannot be explained clearly at this stage, most probably the shape of molecules generated with even spacers is more distorted from the ideal one than that obtained with odd spacers.

Another interesting feature of the cyclic trimers is that some of them exhibit a second mesophase below the nematic phase. The second phase is most probably a smectic A phase according to X-ray diffraction experiments which will be reported elsewhere.[18] The trend of this smectic phase observed for trimers does not seem to be consistent. TPB-(*c*)14(3) and TPB-(*c*)13(3) show a clear second peak on heating and cooling scans of DSC as seen in Figs. 10 and 11. TPB-(*c*)12 trimer shows a similar texture change to that observed for TPB-(*c*)14(3) and TPB-(*c*)13(3) around 47 °C on cooling although its DSC thermogram did not show a clear transition peak. For TPB-(*c*)11(3), TPB-(*c*)10(3), and TPB-(*c*)9(3), neither the change of texture nor the peak in DSC thermograms was observed. The speculative explanation for the presence of a smectic phase in the case of trimers with longer spacers is as follows. Once the spacer length gets close or exceeds the length of the mesogen, the mesogen on an adjacent chain can be staggered, making a rigid molecule. Such a rigid molecule for some reason prefers a smectic phase at a lower temperature. TPB-(*c*)8(3) shows a relatively large second peak which, according to X-ray experiments,[18] corresponds to a transition from the nematic to a smectic phase. However, the speculation mentioned above cannot explain the smectic phase displayed by TPB-(*c*)8(3) and the eventual smectic phase of TPB-(*c*)6(3). Most probably, a different microstructure of the macrocyclic is responsible for the smectic phase displayed by compounds with short spacers.

General Trend of Cyclic Tetramers.—Table 8 summarizes all the data of the cyclic tetramers, TPB-(*c*)*x*(4). Fig. 18a presents

Table 10 Characterization of high relative molecular mass fraction [TPB-(*c*)*x*(*z*)] based on TPB and α,ω-dibromoalkanes containing *x* methylenic units

Spacer length (*x*)	M_n by GPC (M_w/M_n)	Cyclic polymers (mol%)	Thermal transition (°C) and corresponding enthalpy changes (kcal/mru)[a] in parentheses[b]	
			Heating	Cooling
4	6.05×10^3 (1.57)	23	g 83 (−1.21) n 143 (1.64) i g 79 n 143 (1.71) i	i 138 (1.83) n 72 g
5	1.02×10^4 (1.37)	60	g 61 i g 68 i	i 62 g
6	7.24×10^3 (1.60)	63	g 51 n (−0.44) n 131 (2.12) i g 62 n 130 (1.59) i	i 125 (2.07) n 57 g
7	1.01×10^4 (1.40)	27	g 53 n 69 (0.26) i g 53 n 67 (0.10) i	i 62 (0.15) n 48 g
8	8.73×10^3 (1.62)	44	g 42 n 61 (−0.26) n 115 (2.18) i g 47 n 114 (2.12) i	i 109 (2.23) n 42 g
9	1.04×10^4 (1.62)	41	g 48 n 74 (0.54) i g 46 n 73 (0.78) i	i 67 (0.70) n 40 g
10	1.18×10^4 (1.53)	50	g 49 k 57 k 71 n 97 (2.69)[a] i g 28 n 98 (2.31) i	i 89 (2.45) n 24 g
11	7.05×10^3 (1.68)	37	g 44 n 82 (1.07) i g 38 k 55 (0.17) n 81 (0.92) i	i 74 (−0.98) n 47 (0.16) k 34 g
12	6.47×10^3 (1.82)	67	g 41 k 56 (0.45) n 100 (2.59) i g 33 n 101 (2.54) i	i 92 (2.59) n 25 g
13	7.42×10^3 (1.78)	67	g 39 k 45 (0.37) n 79 (1.20) i g 37 k 50 (0.20) n 79 (1.32) i	i 72 (1.24) n 41 (0.31) k 29 g
14	6.12×10^3 (1.67)	58	g 36 k 48 (0.43) k 75 n 85 (4.53)[c] i g 41 k 74 n 84 (4.36)[c] i	i 89 (2.45) n 24 g
18	5.77×10^3 (1.80)	52	g 39 (−0.97) k 84 (5.40) i g 43 k 84 (5.89) i	i 69 (5.36) k 28 g

[a-c] See footnotes in Table 1.

the phase-transition temperatures obtained from the first heating scans of the TPB-(*c*)*x*(4) while Fig. 18b presents the same data obtained from the second heating and first cooling scans. The cyclic tetramers exhibit an enantiotropic nematic phase with a higher tendency toward crystallization than that of the cyclic trimers, especially for the case of longer spacers ($x > 9$). During first heating scans, most of the tetramers exhibit melting or crystallization transitions followed by melting and enantiotropic nematic–isotropic transitions, except for the case of TPB-(*c*)4(4). TPB-(*c*)4(4) tetramer exhibits only a monotropic nematic mesophase. During cooling scans, the tetramers with spacer length shorter than $x = 13$ do not crystallize. TPB-(*c*)13(4) and TPB-(*c*)14(4) show small crystallization peaks which are located in the close proximity of their glass transition. On second heating scans, the tetramers with spacer length shorter than $x = 11$ do not crystallize while those with spacers above $x = 10$ exhibit a crystallization process followed by melting. The longer spacer facilitates the crystallization of the macrocyclics most probably due to their increased molecular flexibility and the better packing ability of the resulting cyclic structure.

Unlike the trimers, the tetramers show a very similar dependence of their nematic–isotropic transition temperatures to that of their associated enthalpy changes *versus* spacer length (Figs. 18 and 19). This trend is similar to that of the linear TPB(*l*)*x* polyethers containing *x* methylenic units in their flexible spacer (Fig. 20).[4] That is, in addition to the odd–even dependence of T_{ni} and T_{in}, there is a continuous decrease of the nematic–isotropic transition temperature for the tetramers and linear polymers with even spacers with increasing spacer length, and a continuous slight increase followed by a slight decrease for the tetramers and linear polymers containing odd spacers (Fig. 20a). This trend is general for any class of molecular[1c-f] and macromolecular[2a,14,17] liquid crystals containing flexible spacers. TPB-(*c*)4(4) is a exception. It exhibits a lower transition temperature and a smaller enthalpy change than that expected from the trend observed for the other tetramers with even spacers. This is most probably due to the fact that the short spacer of TPB-(*c*)4(4) does not allow the proper conformation and alignment of the TPB mesogenic unit. The enthalpy change of the tetramers with both even and odd spacers increases with increasing spacer length and shows a strong odd–even effect which is compared with that of the linear polymers in Fig. 20b. The analogy between the phase behaviour of these cyclic tetramers with that of their linear homologues suggests that there are some similarities of their liquid crystalline phases. Although at least two spacers should have folded to form a cyclic structure, four mesogens and two spacers can adopt almost the same conformation as that of the linear TPB(*l*)*x* as schematically drawn in Scheme 3.

The cyclic tetramers show higher transition temperatures with smaller enthalpy changes than those of their linear homologues[4] (Figs. 20a and 20b). The higher isotropization temperatures of the macrocyclics are most probably due to the lack of chain ends and due to the higher rigidity of the cyclic structure (lower entropy of the structure). The lower enthalpy and entropy changes associated with their nematic–isotropic transitions are attributed to the lower difference between the entropy of the isotropic and liquid crystalline phases of the cyclic structures (Scheme 3). Some additional interesting aspects can be seen from these diagrams. The kinetically prohibited nematic mesophase of the linear polymer [TPB-(*l*)5] which exhibits only a glass transition is transformed into an enantiotropic one [TPB(*c*)5(4)] *via* cyclization. The detailed discussion of this phenomenon was presented elsewhere.[3b] Also, the transformation of a kinetically controlled nematic phase of a linear polymer [TPB-(*l*)7] into a thermodynamically controlled one *via* cyclization was demonstrated in a previous publication.[3c]

General Trend of Cyclic Pentamers.—Table 9 summarizes all the data of the cyclic pentamers, TPB-(*c*)*x*(5). The pentamers again exhibit a nematic phase which displays a very low tendency toward crystallization. The dependences of the nematic–isotropic transition temperatures and of their associ-

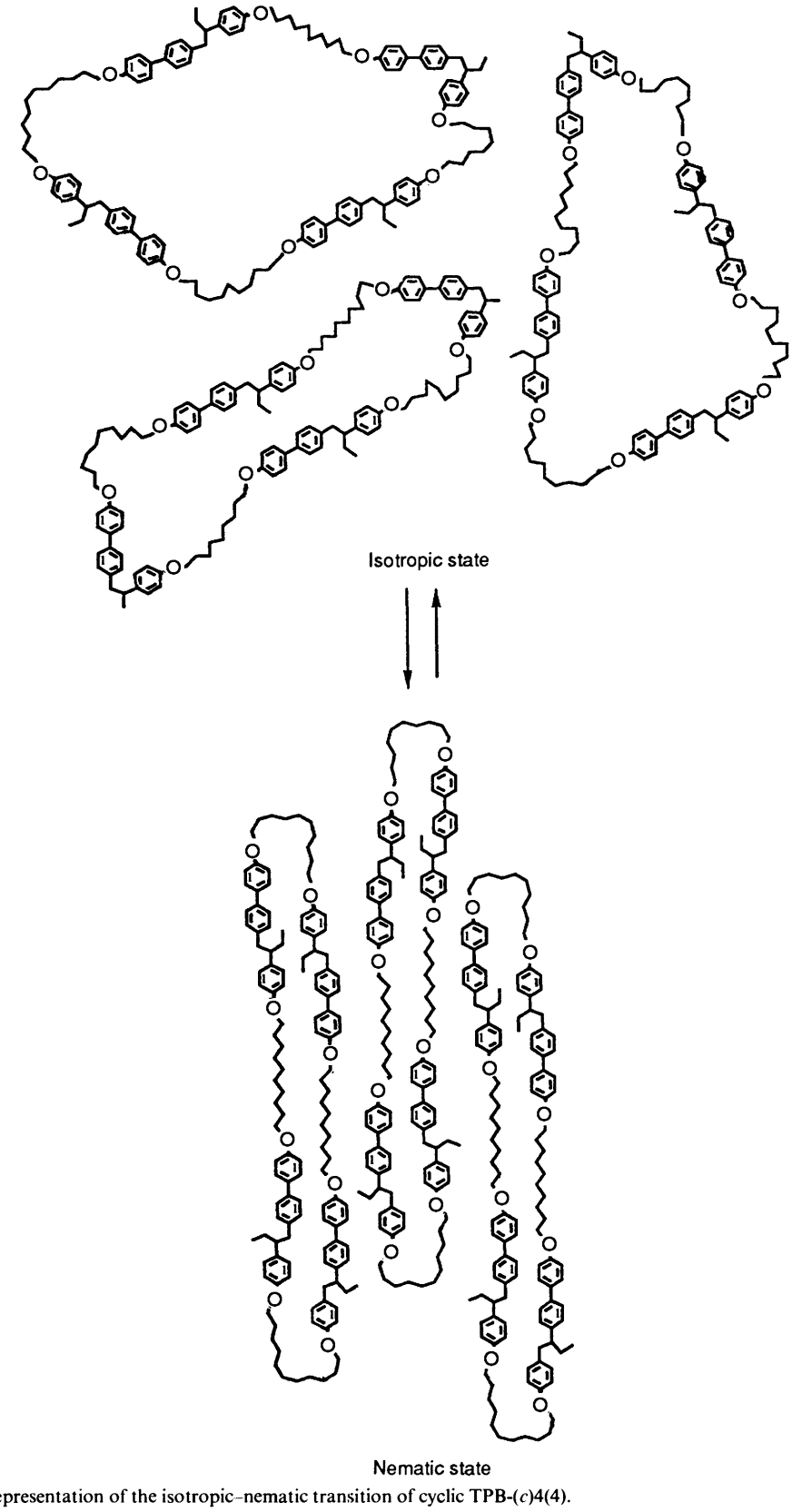

Scheme 3 Schematic representation of the isotropic–nematic transition of cyclic TPB-(*c*)4(4).

ated enthalpy changes on spacer length are quite similar to those of the tetramers (Fig. 21). The larger ring structures again allow the liquid crystalline phase to adopt a similar structure to that of the linear polymers. TPB-(*c*)11(5) shows a second phase which has not yet been identified.

General Trend of the High Relative Molecular Mass Part Eluted with Chloroform.—As discussed in the NMR part, these fractions represent a mixture of linear and cyclic polymers. Their phase behaviour is summarized in Table 10 and is quite similar to that of the high relative molecular mass linear TPB(*l*)*x* series except that the transition temperatures and their corresponding enthalpy changes are slightly lower than those of the linear polymers and their transition peaks are broader in most cases. This is most probably due to both the mixed nature

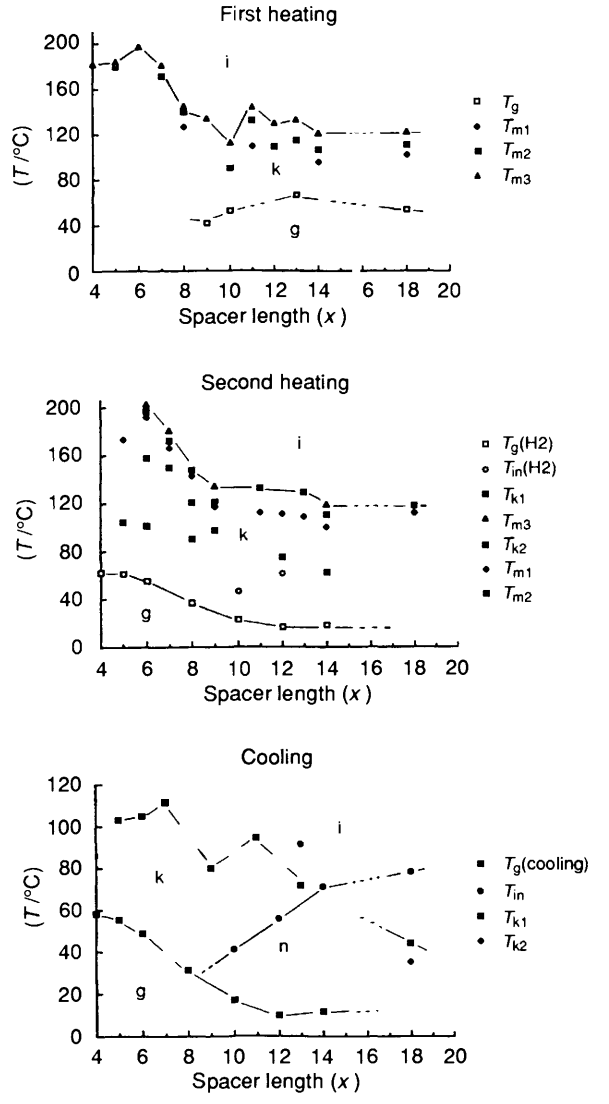

Fig. 15 Transition temperatures of the cyclic dimers *versus* spacer length (x) obtained from: (a) first heating scans; (b) second heating scans; (c) first cooling scans.

of these fractions and to their lower molecular masses. Synthesis of pure, high relative molecular mass macrocyclics is required to elucidate completely their phase behaviour.

Some Considerations of the Odd–Even and Ring Size Effects on the Crystallizability of Macrocyclics.—As discussed above, the crystallization tendency of macrocyclics exhibits an odd–even dependence *versus* ring size. Namely, odd rings display a lower tendency toward crystallization than do even rings. A speculative explanation for this odd–even effect is as follows. The macrocyclics with an even degree of oligomerization, *i.e.*, the dimer and the tetramer, can pack in a crystalline phase containing only the *anti* conformer of the mesogen, while the cyclic oligomers with an odd degree of polymerization, *i.e.*, the trimer and the pentamer, require both the *anti* and the *gauche* conformers of the mesogen in their structure and, therefore, they are less symmetrical if the spacer length is not long enough. This last situation may generate a crystalline phase with a lower degree of order (Scheme 4). Therefore, the cyclic oligomers with an even degree of polymerization may have a lower entropy in the crystalline phase and a higher m.p. than do the cyclic oligomers with an odd degree of polymerization. Elucidation of the crystalline structures of these macrocyclics is nevertheless required in order to confirm this speculative explanation. It is

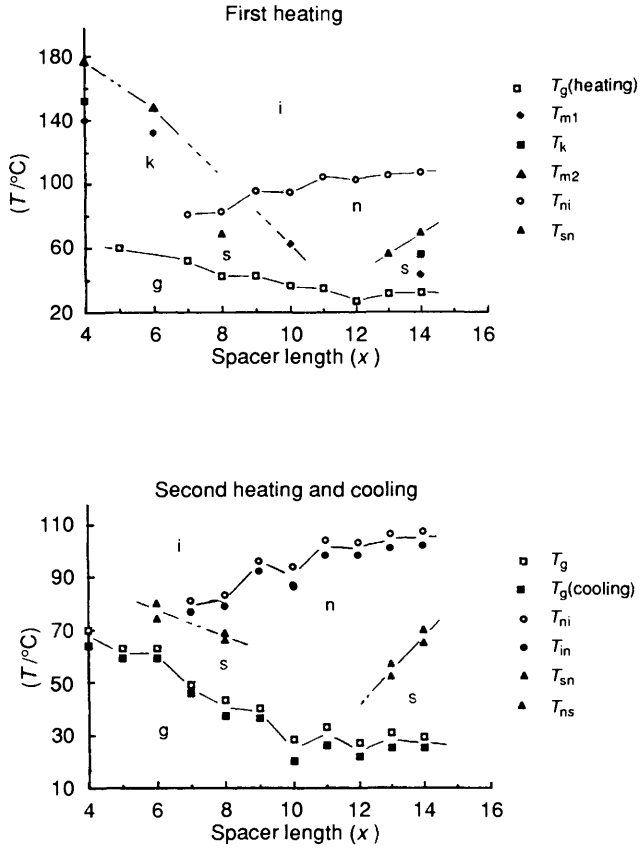

Fig. 16 Transition temperatures of the cyclic trimers *versus* spacer length (x) obtained from: (a) first heating scans; (b) second heating and cooling scans.

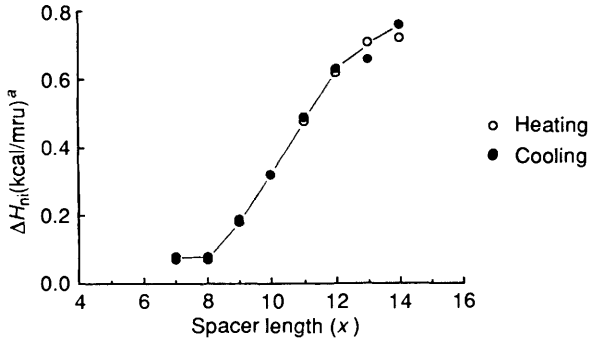

Fig. 17 Enthalpy changes associated with nematic–isotropic transitions of the cyclic trimers *versus* spacer length obtained from second heating and cooling scans.[a] 1 cal = 4.184 J.

interesting that even in the case in which the corresponding homopolymers exhibit a high crystallization tendency, the odd rings exhibit a very low tendency toward crystallization. Therefore, the crystallization tendency of the linear oligomers and polymers is suppressed *via* transformation into macrocyclics containing an odd degree of oligomerization.

Conclusions.—There are some similarities and differences between cyclic oligomers and corresponding high relative molecular mass linear polymers. They can be summarized as follows.

The conformation of the mesogenic unit is highly dependent on the ring size and spacer length in the case of the smaller rings while this is not the case for the larger rings. In the case of the linear polymers the conformation of the mesogenic unit is not affected by the degree of polymerization or by the spacer length.

The cyclic tetramers and pentamers exhibit a nematic meso-

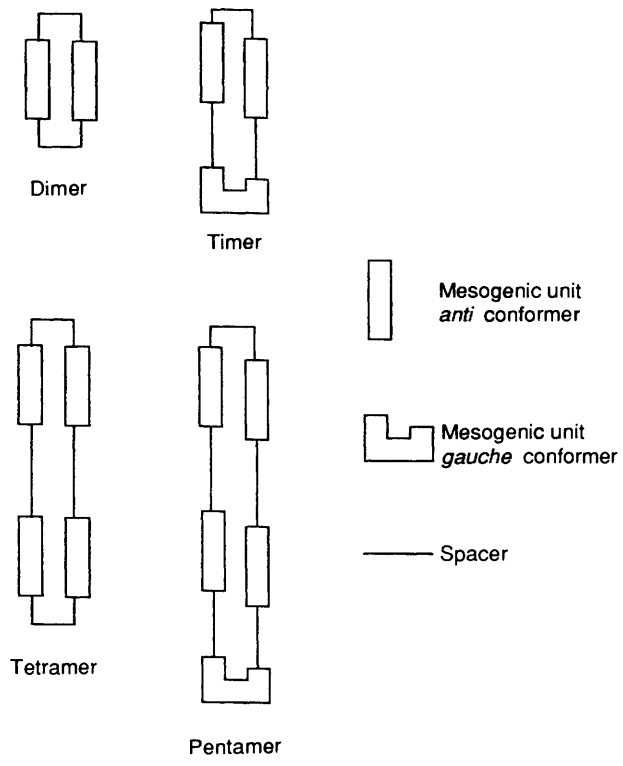

Scheme 4 A possible molecular arrangement of cyclic oligomers in the crystalline phase.

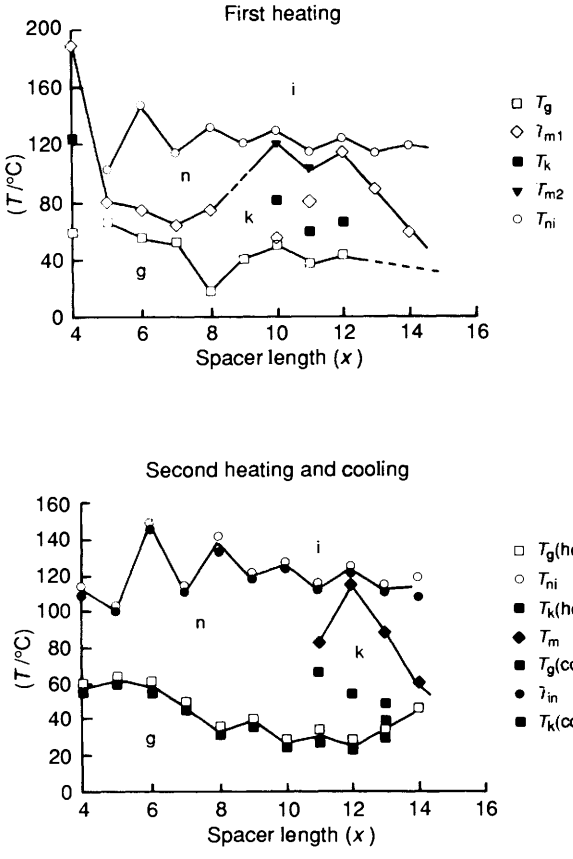

Fig. 18 Transition temperatures of cyclic tetramers *versus* spacer length (x) obtained from (a) first heating scans; (b) second heating and cooling scans.

phase which displays similar odd–even dependences of their isotropization transition temperatures and of their corresponding enthalpy changes on spacer length with those of the

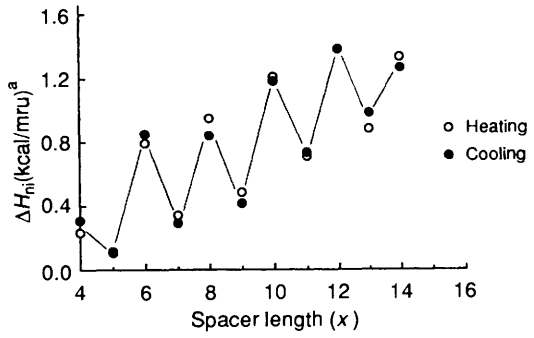

Fig. 19 Enthalpy changes associated with the nematic–isotropic transitions of the cyclic tetramers *versus* spacer length (x) obtained from second heating and cooling scans.[a] 1 cal = 4.184 J.

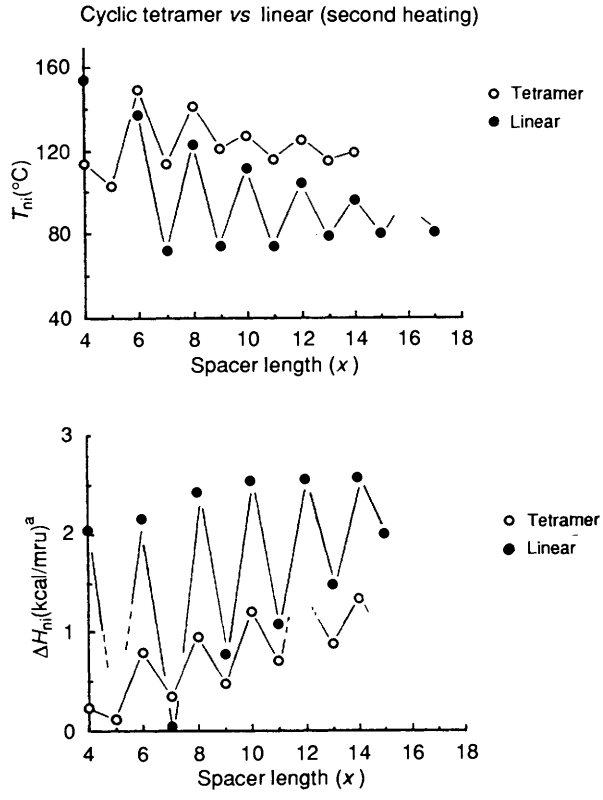

Fig. 20 Comparison of (a) the nematic–isotropic transition temperatures (T_{ni}) and (b) enthalpy changes (ΔH_{ni}) associated with the nematic–isotropic transitions of cyclic tetramers and linear polymers.[a] 1 cal = 4.184 J.

corresponding high relative molecular mass linear polymers. However, their absolute values are different, *i.e.*, the cyclic tetramers and pentamers exhibit higher nematic–isotropic transition temperatures and lower enthalpy changes than do the corresponding high relative molecular mass linear polymers. The cyclic trimers exhibit a weak and inverse odd–even effect of their transition temperatures and enthalpy changes *versus* spacer length. Therefore, the dependence of the transition temperatures and of their thermodynamic parameters on the spacer length is completely different depending on the size and parity of the ring in the case of cyclic oligomers.

Some of the cyclic trimers exhibit a smectic mesophase while none of the corresponding linear polymers exhibit a smectic mesophase. Therefore, macrocyclics exhibit a higher ability to generate smectic mesophases than do their linear homologues. Crystallizability of the high relative molecular mass linear polymers is determined by the spacer length while that of the

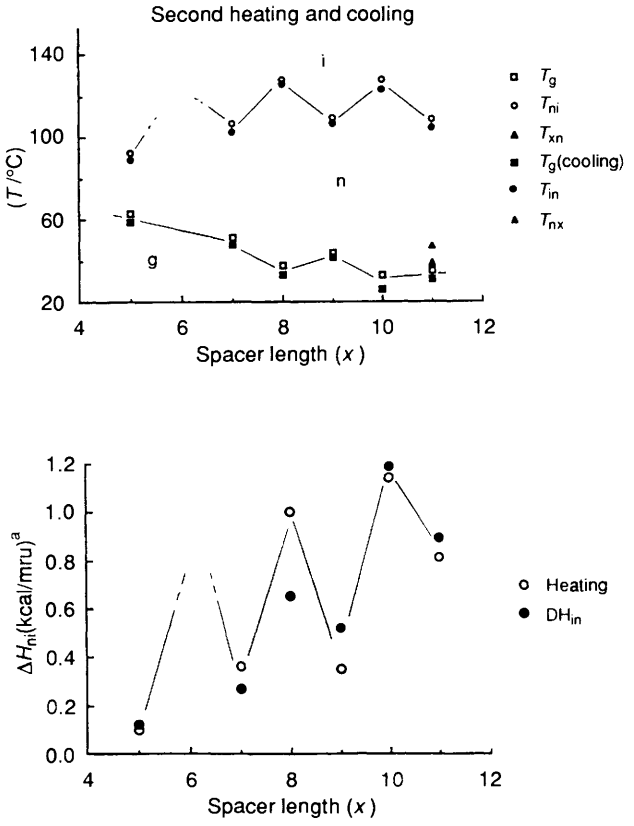

Fig. 21 (a) Transition temperatures and (b) enthalpy changes (ΔH_{ni}) associated with the nematic–isotropic transition of the cyclic pentamers *versus* spacer length (x) obtained from second heating and cooling scans.[a] 1 cal = 4.184 J.

cyclic oligomers is determined by both the spacer length and the parity of the ring size.

Acknowledgements

Financial support by the National Science Foundation, Polymers Program (DMR-92-06781) and Toyota Central R & D Labs., Japan, is gratefully acknowledged.

References

1 (*a*) This is Part 30 in the series: *Liquid Crystalline Polyethers Based on Conformational Isomerism.* For Part 29 see ref. 3*f*; (*b*) F. Reinitzer, *Monatsh. Chem.*, 1888, **9**, 421. An English translation of this paper was published in *Liq. Cryst.*, 1989, **5**, 7; (*c*) D. Vorländer, *Z. Phys. Chem.*, 1923, **105**, 211; (*d*) G. W. Gray, *Molecular Structure and the Properties of Liquid Crystals*, Academic Press, London and New York, 1962; (*e*) in *The Molecular Physics of Liquid Crystals*, eds. G. R. Luckhurst and G. W. Gray, Academic Press, London, 1979, p. 14; (*f*) *Philos. Trans. R. Soc. London., Ser. A*, 1983, **309**, 77; (*g*) *Proc. R. Soc. London, Ser. A*, 1985, **402**, 1; (*h*) H. Kelker and T. Hatz, *Handbook of Liquid Crystals*, Verlag Chemie, Weinheim, 1980; (*i*) D. Demus and H. Zaschke, *Flussige Kristalle in Tabellen*, VEB Deutscher Verlag für Grundstoffindustie, Leipzig, 1984, vol. 2; (*j*) D. Demus, *Mol. Cryst. Liq. Cryst.*, 1988, **165**, 45; (*k*) *Liq. Cryst.*, 1989, **5**, 75.

2 For some recent reviews on macromolecular and supramolecular liquid crystals see: V. Percec and D. Tomazos, (*a*) *Molecular Engineering of Liquid Crystalline Polymers* in *Comprehensive Polymer Science*, 1st Supplement, ed. Sir Geoffrey Allen, Pergamon Press, Oxford, 1992, pp. 300–383; (*b*) *Reactions and Interactions in Liquid Crystalline Media*, in *Polymerization in Organized Media*, ed. C. M. Paleos, Gordon and Breach Scientific Publishers, Philadelphia, 1992, pp. 1–104; (*c*) *Adv. Mater.*, 1992, **4**, 548; (*d*) H. Ringsdorf, B. Schlarb and G. Venzmer, *Angew. Chem., Int. Ed. Engl.*, 1988, **27**, 113.

3 (*a*) V. Percec, M. Kawasumi, P. L. Rinaldi and V. E. Litman, *Macromolecules*, 1992, **25**, 3851; (*b*) V. Percec and M. Kawasumi, *Adv. Mater.*, 1992, **4**, 572; (*c*) *Liq. Cryst.*, 1993, **13**, 83; (*d*) *Mol. Cryst. Liq. Cryst.*, in press; (*e*) *Chem. Mater.*, in press; (*f*) *J. Mater. Chem.*, in press.

4 V. Percec and M. Kawasumi, *Macromolecules*, 1991, **24**, 6318.

5 A. Schneider, J. Blackwell, S. Chvalun, D. Hofmann, G. Ungar, M. Kawasumi and V. Percec, manuscript in preparation.

6 (*a*) V. Percec, C. Pugh, O. Nuyken and S. D. Pask in *Comprehensive Polymer Science*, eds. G. Allen and J. C. Bevington, Pergamon Press, Oxford, 1989, vol. 6, p. 281; (*b*) P. Rempp, C. Strazielle and P. Lutz in *Encyclopedia of Polymer Science and Engineering*, eds. H. F. Mark, N. M. Bikales, C. G. Overberger, G. Menges and J. I. Kroschwitz, Wiley, New York, 2nd edn., 1987, vol. 9, p. 183; (*c*) *Cyclic Polymers*, ed. J. A. Semlyen, Elsevier Applied Science Publishers, New York, 1986; (*d*) P. Knops, N. Sendhoff, H.-B. Mekelburger, F. Vögtle, *Top. Curr. Chem.*, 1991, **161**, 1; (*e*) A. Ostrowicki, E. Koepp and F. Vögtle, *Top. Curr. Chem.*, 1991, **161**, 37; (*f*) J. P. Mathias and J. F. Stoddart, *Chem. Soc. Rev.*, 1992, **21**, 215.

7 (*a*) R. Hilgenfeld and W. Saenger, *Top. Curr. Chem.*, 1982, **101**, 1; (*b*) J. F. Stoddart, *Carbohydr. Res.*, 1989, **12**, 192; (*c*) W. Saenger, *Angew. Chem., Int. Ed. Engl.*, 1980, **19**, 344.

8 (*a*) B. Vollmert and J. X. Huang, *Makromol. Chem., Rapid Commun.*, 1981, **2**, 467; (*b*) D. Geiser and H. Höcker, *Macromolecules*, 1980, **13**, 653; (*c*) J. Roovers and P. M. Toporowski, *Macromolecules*, 1983, **16**, 843; (*d*) J. Roovers, *Macromolecules*, 1985, **18**, 1359; G. Hild, A. Kohler and P. Rempp, (*e*) *Eur. Polym. J.*, 1980, **16**, 525; (*f*) 1983, **19**, 721; (*g*) J. Sundararajan and T. E. Hogen-Esch, *Am. Chem. Soc., Div. Polym. Chem., Polym. Prep.*, 1991, **32**, 604.

9 (*a*) S. J. Clarson and J. A. Semlyen, *Polymer*, 1986, **27**, 1633; (*b*) S. J. Clarson, K. Dodgson and J. A. Semlyen, 1985, **26**, 930; (*c*) C. M. Kuo and S. J. Clarson, *Am. Chem. Soc., Div. Polym. Chem., Polym. Prep.*, 1991, **32**, 595.

10 J. Sundararajan and T. E. Hogen-Esch, *Am. Chem. Soc., Div. Polym. Chem., Polym. Prep.*, 1991, **32**, 63; 1992, **33**, 162.

11 (*a*) D. J. Brunelle, E. P. Boden and T. G. Shannon, *J. Am. Chem. Soc.*, 1990, **112**, 2399; (*b*) D. J. Brunelle and E. P. Boden, *Makromol. Chem., Macromol. Symp.*, 1992, **54/55**, 397 and references cited therein.

12 (*a*) H. M. Colquhoun, C. C. Dudman, M. Thomas, C. A. O'Mahoney and D. J. Williams, *J. Chem. Soc., Chem. Commun.*, 1990, 336; (*b*) M. A. Buese, *Macromolecules*, 1990, **23**, 4341.

13 M. Möller, R. F. Waldron, H. Drotloff, D. Emeis, *Polymer*, 1987, **28**, 1200 and references cited therein.

14 (*a*) V. Percec and B. Hahn, *J. Polym. Sci., Polym. Chem. Ed.*, 1989, **27**, 2367; (*b*) R. D. C. Richards, W. D. Hawthorne, J. S. Hill, M. S. White, D. Lacey, J. A. Semlyen, G. W. Gray and T. C. Kendrick, *J. Chem. Soc., Chem. Commun.*, 1990, 95.

15 For recent reviews and books on various macrocyclics forming host–guest complexes see: (*a*) *Host Guest Complex Chemistry. Macrocyclics*, eds. F. Vögtle and E. Weber, Springer Verlag, New York, 1985; (*b*) L. F. Lindoy, *The Chemistry of Macrocyclic Ligand Complexes*, Cambridge University Press, Cambridge, 1989; J. M. Lehn, (*c*) *Angew. Chem., Int. Ed. Engl.*, 1988, **27**, 89; (*d*) *Angew. Chem., Int. Ed. Engl.*, 1990, **29**, 1304; (*e*) C. D. Gutsche, *Calixarenes*, Royal Society of Chemistry, Cambridge, 1989; (*f*) G. Gokel, *Crown Ethers and Cryptands*, Royal Society of Chemistry, Cambridge, 1991; (*g*) F. Diederich, *Cyclophanes*, Royal Society of Chemistry, Cambridge, 1991.

16 (*a*) For recent reviews on catenands, rotaxanes and knots see: (*a*) C. Dietrich-Buchecker and J. P. Sauvage, *Chem. Rev.*, 1987, **87**, 795; (*b*) J. P. Sauvage, *Acc. Chem. Res.*, 1990, **23**, 319; (*c*) C. Dietrich-Buchecker and J. P. Sauvage, *New J. Chem.*, 1992, **16**, 277; (*d*) D. Philp and J. F. Stoddart, *Synlett*, 1991, 445; (*e*) J. F. Stoddart, *Angew. Chem., Int. Ed. Engl.*, 1992, **31**, 846; (*f*) H. W. Gibson, P. T. Engen, Y. X. Shen, J. Sze, C. Lim, M. Bheda and C. Wu, *Makromol. Chem., Macromol. Symp.*, 1992, **54/55**, 519.

17 V. Percec and Y. Tsuda, *Macromolecules*, 1990, **23**, 3509.

18 V. Percec, M. Kawasumi and G. Ungar, manuscript in preparation.

Paper 3/00193H
Received 12*th January* 1993
Accepted 9*th February* 1993